Journal of South American Earth Sciences 107 (2021) 103092

Contents lists available at ScienceDirect

Journal of South American Earth Sciences

journal homepage: www.elsevier.com/locate/jsames

Geochemical constraints on the origin and distribution of Cretaceous source rocks in the Ceará basin, Brazilian Equatorial margin

Ana Clara B. de Souza [a,*], Daniel R. do Nascimento Jr. [b], Alessandro Batezelli [c], Francisco Nepomuceno Filho [d], Karen M. Leopoldino Oliveira [a], Narelle Maia de Almeida [b], Márcio N. Normando [a], Thiago H. da Silva Barbosa [e]

[a] Programa de Pós-Graduação em Geologia, Universidade Federal do Ceará (UFC), Campus do Pici, Bloco 912, Fortaleza, Ceará, 60440-554, Brazil
[b] Departamento de Geologia, Universidade Federal do Ceará (UFC), Campus do Pici, Bloco 912, Fortaleza, Ceará, 60440-554, Brazil
[c] Departamento de Geologia e Recursos Naturais, Instituto de Geociências – IG; Universidade Estadual de Campinas UNICAMP, Campinas, São Paulo, Brazil
[d] Departamento de Física, Universidade Federal do Ceará (UFC), Campus do Pici, Bloco 922, Fortaleza, Ceará, 60440-554, Brazil
[e] Programa de Pós-Graduação em Engenharia Química, Universidade Federal do Ceará (UFC), Campus 21 do Pici, Bloco 709, Fortaleza, Ceará, 60440-554, Brazil

ARTICLE INFO

Keywords:
Organic geochemistry
Petroleum system
Cretaceous
Hydrocarbon generation
Spatial distribution map

ABSTRACT

The Mundaú sub-basin composes the western segment of the Ceará Basin, which is one of a series of basins of the Brazilian Equatorial Margin that resulted from the breakup of Western Gondwana. This study investigates the origin and maturation of the organic matter preserved in the rocks of the middle and outer shelf of the Mundaú sub-basin, in order to assess the source-rock potential for oil and gas generation. The samples selected for this study are representative of the Mundaú, Paracuru, and Ubarana formations, which correlate with the rift, transition, and drift phases of the Western Gondwana breakup. The results indicate moderate to good potential for oil generation and good potential for gas generation for the Mundaú Formation. Fault activity during the rift phase favored sediment supply. Kerogen type III predominates in shallower portions and probably reflects the contribution from the continent. Good to excellent potential for oil and gas generation is indicated for the Paracuru Formation. Kerogen types I and II predominate, having the marine organic matter been deposited in reducing conditions. The most promising interval for hydrocarbon generation is limited by the top of the Trairí Member and the top of the Paracuru Formation. Moderate to good potential for oil and gas generation is suggested for the Uruburetama Member of the Ubarana Formation. The source rocks located in the middle shelf were deposited under reducing conditions in a transgressive marine environment. Kerogen varies from type II, to a mixture of types II and III, and to subordinate type III. Poor to fair potential for oil generation is indicated for the Itapajé Member of the Ubarana Formation. Kerogen type IV (inert or degraded) is typical in the middle shelf, and kerogen type IV and subordinate type III are typical on the outer shelf. The presence of inert kerogen is related to high-energy, oxidizing depositional environments. The hydrocarbon expulsion threshold estimated for the outer shelf is at 2106-m, for the middle shelf at 1635-m, and for the deep waters at 3632-m depths. Source rocks of the middle and outer shelves occur between 561 m and 4080 m, whereas those in deep waters occur between 2754 m and 5007 m of depth. The Active Source Rock Depth Limits (ASDL) estimated for the outer shelf is below 4500 m, whereas for deep waters, this limit is close to 6000 m. These organic geochemical constraints are important guidelines for oil and gas exploration in the Ceará and adjacent basins.

1. Introduction

The characterization of source rocks in petroleum geology includes the quantification and qualification of the organic matter present in them and the determination of their potential to generate hydrocarbons (Espitalié et al., 1977; Katz, 1983; Tissot and Welte, 1984; Anders, 1991; Jarvie, 1991; Hunt 1995; Dembicki, 2009; Hart and Steen, 2015). Fine-grained siliciclastic rocks, such as shales, mudstones, and siltstones,

* Corresponding author.
E-mail addresses: anaclarageologia@alu.ufc.br, souzaanaclarageologia@gmail.com (A.C.B. Souza), daniel.rodrigues@ufc.br (D.R. Nascimento), abatezelli@ige.unicamp.br (A. Batezelli), nepomuceno@fisica.ufc.br (F. Nepomuceno Filho), karenleopoldino@gmail.com (K.M. Leopoldino Oliveira), narelle@ufc.br (N. Maia de Almeida), thiagohenrique@alu.ufc.br (T.H.S. Barbosa).

https://doi.org/10.1016/j.jsames.2020.103092
Received 9 August 2020; Received in revised form 10 November 2020; Accepted 4 December 2020
Available online 24 December 2020

are the largest oil deposits of the Earth's sedimentary record (e.g., Aplin and Macquaker, 2011). In a conventional petroleum system, they can work either as source or seal rocks (Magoon and Dow, 1994). The spatial distribution, quality, and oil content of these rocks are critical features in assessing exploratory risks (Cornford, 1979; Tissot and Welte, 1984; Curiale et al., 1992; Peters and Cassa, 1994; Harris, 2005; Peters et al., 2007; Curiale, 2008). Organic geochemical data provide information regarding the type of organic matter, its thermal maturity, and the potential threshold for hydrocarbon generation and expulsion (e.g., Katz, 1983; Dembicki, 2009; Hart and Steen, 2015). Thus, the geochemical approach provides critical information to assess a petroleum system (e.g., Katz, 1983; Peters et al., 2007; Dembicki, 2009).

Globally, Cretaceous petroleum systems contain significant source rocks (Peters et al., 1993). The economic relevance of the Aptian–Turonian organic-rich sediments is attested worldwide since they include more than 29% of the recoverable hydrocarbon (oil and gas) reserves (e.g., Kolonic et al., 2005). In the Ceará Basin, located in the Brazilian Equatorial Margin, organic-rich strata occur in Aptian-Albian successions. Shales, mudstones, siltstones, sandstones, limestones, and minor evaporites make up the regarded as high-quality source rocks of the Equatorial Margin (Condé et al., 2007; Pellegrini and Ribeiro, 2018).

In a broad sense, the deposition of organic-rich shales in the Brazilian Equatorial Margin (e.g., Ceará, Potiguar, Barreirinhas, and Pará-Maranhão basins) is a consequence of regional and tectonic events of organic matter accumulation (Condé et al., 2007; Pessoa Neto et al., 2007; Trosdtorf Jr. et al., 2007). However, these potential source rock successions lack geochemical studies showing their spatial distribution, the origin of organic matter, degree of maturation, and burial history. This study aims to present an evolutionary model for the main petroleum systems of the Mundaú sub-basin, part of the Ceará Basin, by means of organic geochemical analysis. Additionally, this information is used to unravel the relationship between source rocks and (i) shelf and deep-water domains within the Mundaú sub-basin; (ii) neighboring, closely-related Brazilian Equatorial Margin basins; and (iii) Equatorial Conjugate Margins of Africa.

2. Regional geology

The Ceará Basin is located in Northeastern Brazil and belongs to a series of offshore basins of the Brazilian Equatorial Margin (Fig. 1A) that border the states of Ceará, Piauí, and the Maranhão. The Fortaleza and Tutóia Highs separate the Ceará Basin from the Potiguar and Barreirinhas basins (Mohriak and Rosendahl, 2003). The south limit is marked by Precambrian rocks of the Borborema Province (Costa et al., 1990), whereas in the north limit two tectonic and geomorphologic features stand out: (i) the Romanche Fracture Zone, which stretches out to an expressive fault locally known as the Ceará Transform Fault; and (ii) the Ceará Guyot, a volcanic feature that is considered as an extension of the Fernando de Noronha Chain (Costa et al., 1990) (Fig. 1B).

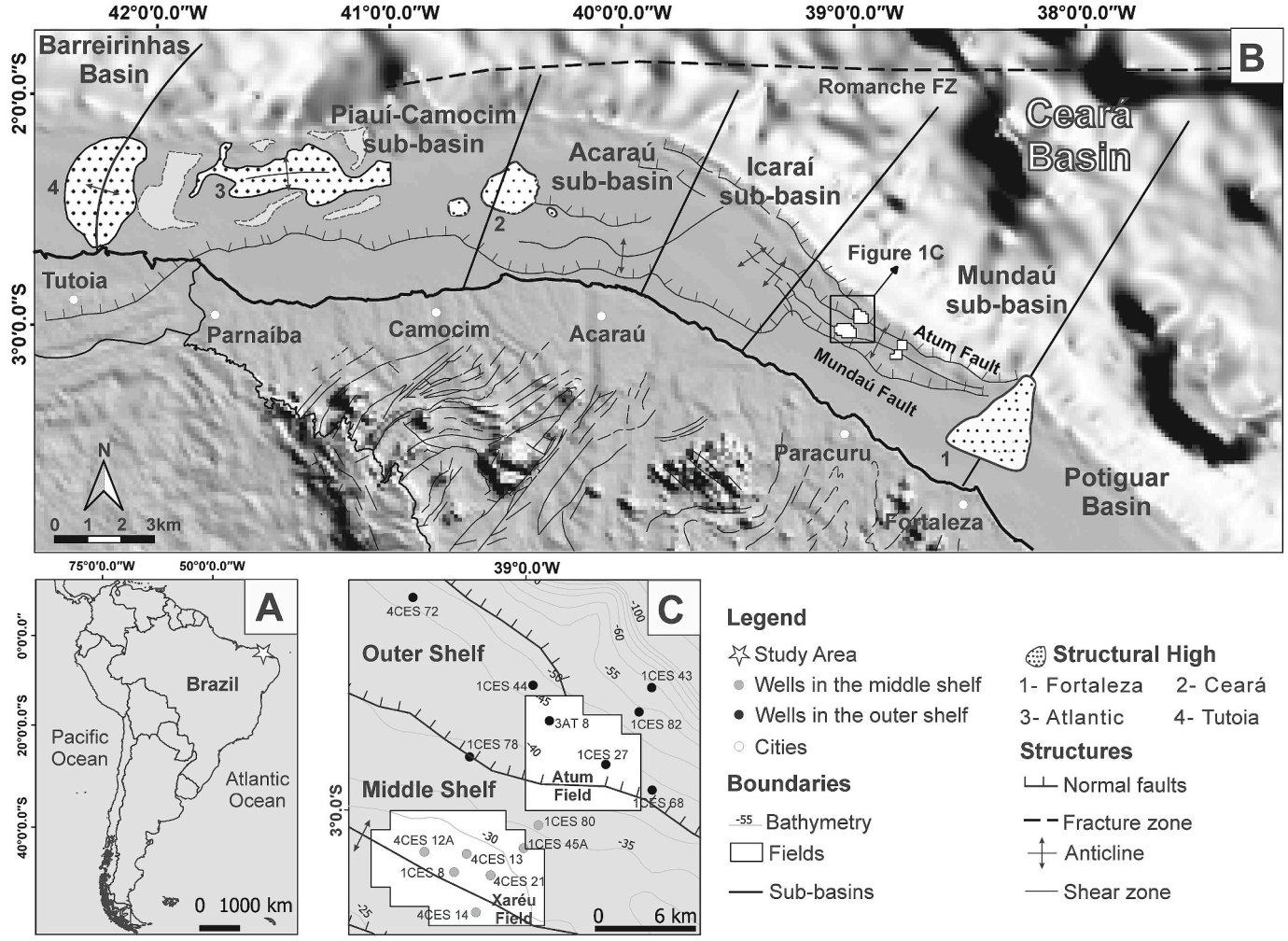

Fig. 1. Location of the Ceará Basin in South America. B) Structural elements of the study area, highlighting fault boundaries (the Mundaú and Atum faults), the extension of major intrusive structures and contacts between the four Ceará sub-basins (Modified after Morais Neto et al., 2003 and Silva Filho et al., 2007). C) Location of the 15 wells in the middle shelf and the outer shelf selected for this study.

The Ceará Basin is subdivided into the Mundaú, Icaraí, Acaraú and Piauí-Camocim sub-basins (Fig. 1B), which originated under different tectonic-sedimentary regimes (Zalán et al., 1985; Costa et al., 1990; Morais Neto et al., 2003; Condé et al., 2007). This subdivision helped individualize two main segments in the Ceará Basin, characterized by different structural and stratigraphic styles. The eastern segment, which includes the Piauí–Camocim, Icaraí, and Acaraú sub-basins, is characterized by E-W-trending compressional and extensional tectonic structures. The western segment is composed of the Mundaú sub-basin, characterized by a series of tilted blocks limited by normal faults striking NW-SE and dipping NE (Azevedo, 1991; Maia de Almeida et al., 2020b; Leopoldino Oliveira et al., 2020). The shelf domain is divided in three areas according to sedimentological and morphological patterns: the up to 20 m-deep inner shelf; the 20 to 40 m-deep middle shelf; and the more than 40 m-deep outer shelf, which extends to the shelf break (Coutinho and Morais, 1968). The database available for the Mundaú sub-basin helps distinguish a proximal region or middle shelf, and a distal region or outer shelf (Fig. 1C).

The origin and evolution of the Ceará basin is a consequence of the breakup of the Western Gondwana supercontinent in the Lower Cretaceous (Almeida et al., 2000) and of the non-simultaneous opening of the Equatorial and South Atlantic oceans, which resulted in a series of on- and offshore Mesozoic-Cenozoic basins, distributed over 2200 km along the present South Atlantic (Matos, 2000). As described by Davison et al. (2016) and summarized here, in the early Aptian, the transtensional rift phase of the Equatorial Atlantic opening produced deep, E- to ENE-trending graben filled with non-marine sediment along the Romanche Fracture Zone in the Barreirinhas and Togo-Benin basins (Azevedo, 1991; Mascle et al., 1988; Matos, 2000). Both E-W-trending strike-slip faults and NE- to ENE-trending transtensional faults were produced during the rifting, defining a *ca.* 140 km-wide transtensional rifted corridor. Rifting continued into the early Albian and, by late Albian times, a deep marine environment had developed (Matos, 2000). Ocean spreading initiated at approximately 110 Ma (Heine and Brune, 2014). A change in plate-movement vectors must have occurred near the end of the Albian, which resulted in dextral transpression of the rifted margin (Szatmari et al., 1987; Azevedo, 1991) and produced a matching pair of fold and thrust belts on the African and South American margins. The two fold belts were then separated by the continued opening of the Equatorial Atlantic Ocean.

The Mundaú sub-basin not only gathers the major oil and gas exploration activities, but also the thickest and most complete sedimentary record of the Ceará Basin (Condé et al., 2007). The tectonic-sedimentary evolution of the Mundaú sub-basin took place in three main stages: rift (continental), post-rift (transitional), and drift (open-marine) (Szatmari et al., 1987) (Fig. 2). The Mundaú Formation (Costa et al., 1990) is the basal unit of the Ceará Basin, formed during a rift phase in the Early Aptian – Alagoas Local Stage (Fig. 2). It is composed of continental sediments deposited in alluvial, lacustrine, and fluvial depositional systems. The top of the Mundaú Formation configures a regional unconformity named Mark 100 (Beltrami et al., 1994; Pessoa Neto, 2004).

The Paracuru Formation overlies the Mundaú Formation and is a transitional sequence deposited from the Neoaptian to the Early Albian (Costa et al., 1990; Beltrami et al., 1994; Condé et al., 2007) (Fig. 2). Sandstones and bioturbed grayish shales compose the lower interval of this formation (Beltrami et al., 1994; Morais Neto et al., 2003; Condé et al., 2007). The middle interval, also known as the Trairí Member, includes carbonaceous shales with ostracods and calcilutites. A restrict halite deposit in the Trairí Member is the only known evaporite occurrence in the Ceará Basin (Hashimoto et al., 1987; Regali, 1989) (Fig. 2). The top of the Paracuru Formation is composed of shales and minor occurrences of calcilutites and fine-grained sandstones (Beltrami et al., 1994; Condé et al., 2007).

In a general view, the depositional environment of the Paracuru Formation evolved from deltaic to marginal *sabkha*, and then to restricted marine (Beltrami et al., 1994). The late interval of the Paracuru Formation records the first marine ingression in the Ceará Basin, and the transition from continental to marine environments characterizes the breakup sequence (Mohriak and Rosendahl, 2003; Maia de Almeida et al., 2020a; Leopoldino Oliveira et al., 2020).

The drift phase of the Ceará Basin corresponds to sediments deposited on an unconformity on top of the Paracuru Formation, which characterize shallow and deep marine sedimentation (Condé et al., 2007). This succession extends from the Albian to the Holocene and is divided into the Ubarana, Tibal, and Guamaré formations. The Ubarana Formation is composed of two distinct members (Fig. 2): The Uruburetama Member, which is a transgressive marine sequence represented by shales and siltstones deposited from the Albian to the Eocampanian (Lana et al., 2002), and the Itapajé Member, which corresponds to a regressive cycle and is composed of shales, turbidite sandstones, and calcilutites deposited from the Neocampanian to the Holocene. As a whole, the Ubarana Formation is laterally associated and interlayered with the shelf carbonates from the Guamaré Formation (Mohriak and Rosendahl, 2003) and with the transitional sandstones of the Tibau Formation (Beltrami et al., 1994).

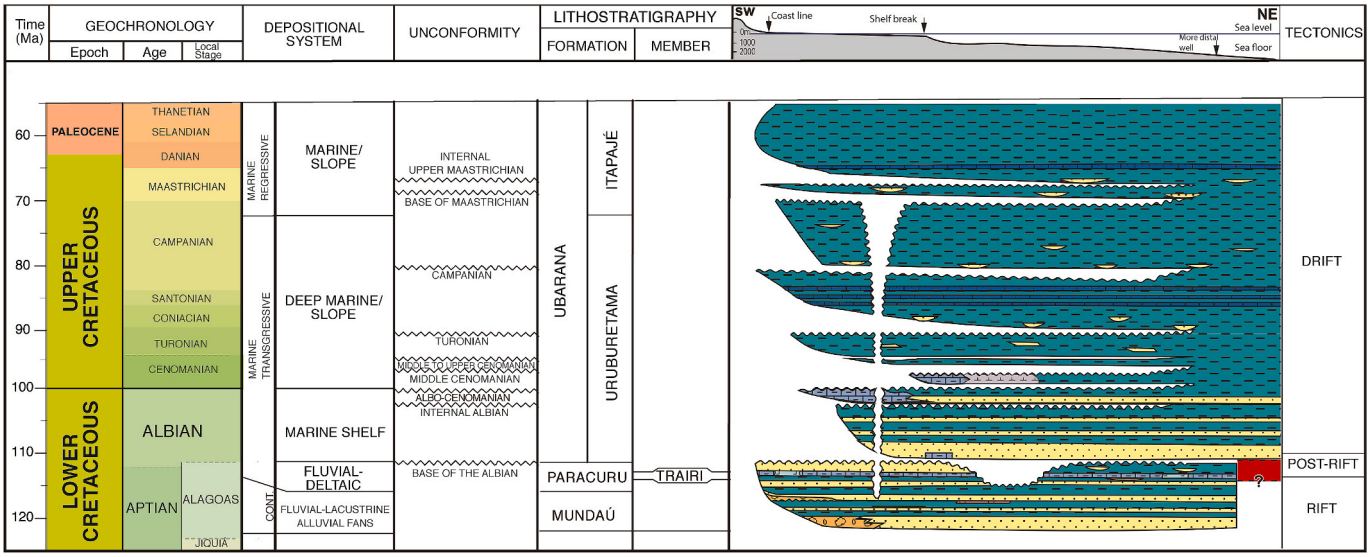

Fig. 2. Simplified stratigraphic chart of the Ceará Basin (extracted from Condé et al., 2007).

The petroleum systems of the Ceará Basin are related to all tectonic phases of its evolution (Beltrami et al., 1994). Despite the relative scarcity of geochemical data, which are mostly recorded in internal reports from oil companies (e.g., Mello et al., 1984; Mello et al., 1988), some authors (Costa et al., 1990; Pessoa Neto, 2004) highlight the shales of the Paracuru Formation marine-evaporitic sequence as significantly potential source rocks for oil and gas. Previous works report kerogen types I and II and high TOC contents for these rocks, attesting their excellent potential (Cerqueira et al., 1994). Likewise, the shales of the Mundaú Formation are considered potential source rocks, once deposition took place in a lacustrine environment. The mean TOC content of 2% is an indication of fair to excellent potential (ANP, 2017).

3. Data and methods

3.1. Available database

Fifteen exploratory wells were selected for the present study, seven of which are located in the middle shelf or proximal region (close to the Xaréu field) and eight in the outer shelf or distal region (close to the Atum field) (Figs. 1C, 12 and 13). The Brazilian Agency for Petroleum, Natural Gas and Biofuels (ANP) provided the geochemical dataset for a total of 1571 core samples selected from the exploratory wells. The dataset includes the analysis of total organic carbon (TOC), vitrinite reflectance (Ro), and Rock-Eval pyrolysis indexes (free hydrocarbons–S1, hydrocarbon generative potential–S2, hydrogen index–HI, oxygen index–OI, temperature at the maximum of the S2 peak–T_{max}) (Tables 1 and 2). These parameters were imported to the Petrel E&P® software platform with permission of use granted to the Federal University of Ceará (UFC).

3.2. Geochemical information

The methods usually applied in source rock evaluation are Total Organic Carbon, Rock-Eval Pyrolysis, and Vitrinite Reflectance (Jarvie, 1991) and are discussed below.

3.2.1. Total organic carbon (TOC)

The amount of organic matter in source rocks is fundamental for the generation of hydrocarbons (Tissot and Welte, 1984). Therefore, the determination of the carbon content is a priority in source-rock evaluation. The TOC technique provides semi-quantitative information on the organic matter contained in a sample. It also represents the biogenically-derived carbon and reflects the production and preservation conditions in a depositional environment (Espitalié et al., 1977; Jarvie, 1991; Hart and Steen, 2015), and is one of the first and most important parameters to be obtained for the evaluation of oil shales (e.g., Hunt, 1995).

The amount of organic matter present in sediment or rock samples is obtained by a direct combustion technique that requires only 1 g of powdered sample. The sample to be analyzed is pulverized and treated so as to remove any inorganic carbon. It is then combusted at 1200 °C. Kerogen carbon is converted to CO and CO_2, which are collected and analyzed (Peters and Cassa, 1994). The carbon fraction is measured and the resulting value is converted to TOC and recorded as weight percent (wt.%). A TOC analyzer is used to determine TOC and additional parameters, such as pyrolyzed carbon (PC, %), insoluble residue (IR, %), and residual carbon (RC, %) (e.g., Hunt, 1995; Jarvie, 1991; Katz, 2005).

3.2.2. Rock-Eval pyrolysis

The Rock-Eval Pyrolysis simulates the natural conditions of organic matter metagenesis and catagenesis, yielding parameters for source-rock evaluation. During pyrolysis, the samples are heated under an inert atmosphere of helium or nitrogen. A flame ionization detector senses organic compounds emitted during each stage of heating, while sensitive infrared detectors measure CO and CO_2 during pyrolysis and oxidation (Espitalié et al., 1977; Bordenave et al., 1993). The parameters provided by the analysis are:

Table 1
Minimum (Min.), maximum (Max.) and mean (Avg.) values of the geochemical parameters TOC, and IR, including S1, S2, S3 and T_{max} obtained from Rock-Eval pyrolysis, and calculated parameters HI, OI, Ro, GP, PI and RHP for core sample sets selected from the seven wells located in the middle shelf of the Mundaú sub-basin (see Fig. 1C).

Stratigraphic unit		TOC	IR	S1	S2	S3	T_{max}.	HI	OI	$Ro_{(calc)}$	GP	PI	RHP
Itapajé Mb.	Min.	0.30	20.00	0.01	0.29	0.78	414.00	28.43	46.55	0.29	0.31	0.02	0.33
	Max.	3.39	92.00	1.69	6.68	4.00	440.00	575.86	262.26	0.76	8.37	0.50	7.22
	Avg.	0.74	84.00	0.17	0.85	1.80	423.00	75.23	199.46	0.45	1.16	0.15	0.97
	#samples	106	31	31	31	31	31	31	31	31	31	31	31
Uruburetama Mb.	Min.	0.70	48.00	0.01	0.21	0.88	411.00	22.34	48.45	0.24	0.34	0.01	0.36
	Max.	1.94	89.00	1.32	2.79	3.57	434.00	192.41	323.40	0.65	3.15	0.45	2.48
	Avg.	1.12	81.73	0.17	1.17	1.93	426.45	91.55	162.23	0.52	1.33	0.12	1.05
	#samples	41	29	29	29	29	29	29	29	29	29	29	29
Paracuru Fm.	Min.	0.13	52.00	0.01	0.26	0.06	390.00	26.26	3.44	0.15	0.28	0.00	0.28
	Max.	9.27	96.00	4.64	62.92	4.81	457.00	781.04	280.41	1.07	64.56	0.41	8.07
	Avg.	1.15	82.00	0.16	2.17	1.08	431.00	161.90	71.11	0.60	2.31	0.07	1.67
	#samples	357	297	297	297	297	297	297	297	297	297	297	297
Mundaú Fm.	Min.	0.58	63.00	0.01	0.25	0.21	424.00	22.81	7.97	0.47	0.31	0.01	0.29
	Max.	5.18	92.00	1.54	30.35	12.68	455.00	585.91	868.49	1.03	31.42	0.41	6.07
	Avg.	1.08	84.00	0.17	1.62	0.71	436.00	109.71	56.85	0.69	1.83	0.09	1.23
	#samples	156	136	118	118	118	118	118	118	118	118	118	118

TOC: Total organic carbon, wt.%.
IR: Insoluble residual, wt.%.
S1: Volatile hydrocarbon HC content, mg HC/g rock.
S2: Remaining HC generative potential, mg HC/g rock.
S3: Carbon dioxide content, mg CO_2/g rock.
T_{max}: Temperature at maximum of S2 peak (°C).
HI: Hydrogen Index = S2 x 100/TOC, mg HC/g TOC.
OI: Oxygen Index = S3 x 100/TOC, mg CO_2/g TOC.
Ro(calc): vitrinite reflectance calculated = $0.018 \times T_{max} - 7.16$.
PI: production index = S1/(S1 + S2).
GP genetic potential = S1+ S2, mg HC/g rock.
RHP: relative hydrocarbon potential = (S1 + S2)/TOC.

Table 2
Minimum (Min.), maximum (Max.) and mean (Avg.) values of the geochemical parameters TOC, and IR, including S1, S2, S3 and T_{max} obtained from Rock-Eval pyrolysis, and calculated parameters HI, OI, Ro, GP, PI and RHP for core sample sets selected from the eight wells located in the outer shelf of the Mundaú sub-basin (see Fig. 1C).

Stratigraphic unit		TOC	IR	S1	S2	S3	T_{max}.	HI	OI	$Ro_{(calc)}$	GP	PI	RHP
Itapajé Mb.	Min.	0.08	38.00	0.02	0.23	0.26	407.00	31.21	20.89	0.17	0.31	0.01	0.35
	Max.	4.93	96.00	1.94	14.62	6.41	456.00	335.32	475.00	1.05	16.45	0.47	3.96
	Avg.	1.72	77.00	0.25	1.72	2.15	427.00	89.95	117.13	0.53	2.02	0.13	1.04
	#samples	279	250	250	250	250	250	250	250	250	250	250	250
Uruburetama Mb.	Min.	0.45	60.00	0.02	0.12	0.34	417.00	16.44	20.09	0.35	0.22	0.01	0.30
	Max.	4.47	92.00	1.73	16.67	2.89	440.00	636.26	444.83	0.76	18.40	0.45	7.02
	Avg.	1.47	80.17	0.49	4.50	1.48	429.63	258.41	105.78	0.57	4.98	0.11	2.88
	#samples	158	132	132	132	132	131	132	132	131	132	132	132
Paracuru Fm.	Min.	0.06	5.00	0.01	0.22	0.01	414.00	25.84	1.16	0.29	0.00	0.00	0.38
	Max.	16.20	98.00	4.77	52.68	3.58	463.00	941.85	339.08	1.17	55.76	0.43	9.67
	Avg.	1.17	84.00	0.21	1.69	0.68	435.00	136.34	39.22	0.67	1.91	0.10	1.64
	#samples	406	338	338	338	338	338	338	338	338	345	338	338
Mundaú Fm.	Min.	0.61	79.00	0.03	0.40	0.11	430.00	41.50	6.21	0.58	0.48	0.04	0.53
	Max.	2.85	92.00	1.89	5.85	0.91	463.00	269.10	103.41	1.17	7.34	0.66	3.12
	Avg.	1.10	87.00	0.24	1.21	0.32	448.00	119.79	26.71	0.90	1.57	0.13	1.46
	#samples	68	57	57	57	57	57	57	57	57	57	57	57

TOC: Total organic carbon, wt.%.
IR: Insoluble residual, wt.%.
S1: Volatile hydrocarbon HC content, mg HC/g rock.
S2: Remaining HC generative potential, mg HC/g rock.
S3: Carbon dioxide content, mg CO_2/g rock.
T_{max}: Temperature at maximum of S2 peak (°C).
HI: Hydrogen Index = S2 x 100/TOC, mg HC/g TOC.
OI: Oxygen Index = S3 x 100/TOC, mg CO_2/g TOC.
Ro(calc): vitrinite reflectance calculated = $0.018 \times T_{max} - 7.16$.
PI: production index = S1/(S1 + S2).
GP genetic potential = S1+ S2, mg HC/g rock.
RHP: relative hydrocarbon potential = (S1 + S2)/TOC.

1. Free hydrocarbons within the organic matter – S1 (mg HC/g rock);
2. Amount of hydrocarbons generated by thermal cracking – S2 (mg HC/g rock);
3. Amount of CO_2 released during pyrolysis, which is proportional to the oxygen present in the kerogen – S3 (mg CO_2/g rock), and
4. The temperature of the maximum peak of S2 – T_{max} (°C).

The parameters or indexes calculated using S1, S2, S3 and T_{max} are: A) The hydrogen index (HI), expressed in milligrams of hydrocarbons (HC) per gram of TOC. It is used to characterize the origin and maturity of the kerogen of organic matter. HI values typically range from ~100 to 600 mg HC/g TOC and are related to the hydrogen to carbon ratio (H/C). B) The oxygen index (OI), also expressed in milligrams of hydrocarbons per gram and ranging from 0 to ~150 mg HC/g TOC. It is a parameter that correlates with the oxygen to carbon ratio (O/C). C) The genetic potential (GP) is the sum of the values S1 and S2 (mg HC/g rock), and the D) Production index (PI) is used to characterize the evolution level of the organic matter (Barker, 1974; Espitalié et al., 1977, 1984; Jarvie, 1991; Hart and Steen, 2015). These indexes are calculated as follows: HI = S2/TOC x 100 (mg HC/g TOC); OI = S3/TOC x 100 (mg CO_2/g TOC); GP = S1 + S2 (mg HC/g rock), and PI = S1/[S1+S2] (Behar et al., 2001).

The parameters were plotted in discriminant diagrams, in order to identify organic matter types (S1 vs. TOC), kerogen type (HI vs. OI, which is called here Van Krevelen diagram, as it replaces the atomic H/C vs. O/C), maturity (HI vs. T_{max}), and quality (S2 vs. TOC) (Van Krevelen, 1961; Peters, 1986; Espitalié et al., 1984; Tissot and Welte, 1984; Langford and Blanc-Valleron, 1990; Peters and Cassa, 1994; Jarvie, 2012). Kerogen type and maturity diagrams are commonly used to define different maturity windows (e.g., immature, oil window, condensate wet gas zone, dry gas window).

Thus, organic matter type, maturity, and nature of source rocks are fundamental to understand the relationship between these parameters and depositional environment (Tissot and Welte, 1984). In this sense, Tissot and Welte (1984) and Peters et al. (2006) describe four kerogen types, as described below:

1 Type I – oil prone. This kerogen is mostly derived from lacustrine algal and bacterial matter (marine/terrestrial environment), although kerogen type I may be predominant in certain source rocks deposited in marine environments.
2 Type II – oil and gas prone. It is the most common type of kerogen in source rocks that have stored conventional hydrocarbon accumulations. It is usually related to marine organic matter, indicating the deposition of autochthonous algal and bacterial material, with medium to high sulfur content, in addition to pollens, spores and cuticles of land plants. The source rocks were mostly deposited in reducing environments.
3 Type III – gas prone. Kerogen is widely derived from plant matter. It indicates an origin in terrestrial environments, such as swamps, lagoons, and deltas. Generally, oxygen contents are higher when compared to those of kerogen types I and II.
4 Type IV – neither oil nor gas prone (inert). HI values are low, typical of oxidized or reworked organic matter.

Two additional parameters were calculated for this study: the relative hydrocarbon potential (RHP) and the active source rock depth limits (ASDL). The relative hydrocarbon potential (RHP = [S1+S2]/TOC) (Fang et al., 1993) was used in addition to the classical geochemical data treatment (e.g., Van Krevelen diagrams) because, when RHP is associated with depth, it is possible to discuss hydrocarbon generation and expulsion. Based on the RHP index, Pang et al. (2005) proposed a conceptual model in which a Hydrocarbon Generation Threshold (HGT) is established when the RHP index continually decreases after a maximum is reached (Fujie et al., 2016; Xu et al., 2019; Tang et al., 2019). Hydrocarbon generation can be understood as a process of deoxidation, dehydrogenation, and carbon enrichment (Peters and Cassa, 1994). Thus, this process is expressed by decreases in atomic H/C and O/C ratios (Tissot and Welte, 1984) As hydrocarbons are gradually

generated, hydrogen and oxygen contents progressively decrease in the organic matter. This relationship also applies to ASDL (Pang et al., 2019). The active source rocks are organic-rich sedimentary rocks capable of generating hydrocarbons. Pang et al. (2019) define the ASDL index as the maximum burial depth of active source rocks beyond which the source rocks no longer generate or expel hydrocarbons and become inert. ASDL helps identify the maximum depth of distribution of fossil fuel resources.

3.2.3. Vitrinite reflectance (VR)

Vitrinite reflectance values (%Ro) were available for exploratory well 1-CES-8 (Fig. 11 – see transect represented by the orange line). Vitrinite reflectance is the most widely used method to determine the thermal maturity of the organic matter. This technique measures the light reflectance from polished vitrinite maceral surfaces coated with immersion oil, and was initially developed to analyze coal under the microscope and later applied to kerogen (Jacob, 1989). Ro values can be calculated using T_{max} data and the formula developed by Jarvie and Lundell (2001):

$$Ro_{calc} = (0.0180 \times T_{max}) - 7.16$$

3.3. Spatial analysis

For the spatial analysis, transects and isoline maps were drawn using data from the logs of the 15 exploratory wells selected for this study (seven in the middle shelf and eight in the outer shelf), as shown in Fig. 1C.

The transects enabled lateral correlations of thickness, facies, and geochemical data (TOC, HI, RHP, and T_{max}). The rock types represented by the 1571 core samples chosen from the 15 wells include black to medium-gray shales, siltstones, mudstones, and other fine-grained rocks. The top of the lithostratigraphic unit represented by these samples is indicated by numbered lines in Figs. 11 and 12.

The isoline maps for each stratigraphic unit (Figs. 13–17) represent the areal distribution of the geochemical parameters TOC, GP, HI, and T_{max}. These maps were produced by the Petrel software platform by means of the convergent interpolation algorithm. The surface resulting from the application of such algorithm is a more realistic representation in areas of complex geology (Babakhani, 2018). Approaches similar to the one adopted here can be found in Rullkötter et al. (1982), Li et al. (1997), Peters and Cassa, 1994, Peters et al. (2006) Peters et al. (2007), Omodeo-Salé et al. (2016) and Xu et al. (2019), among others.

4. Results and interpretations

When analyzing the oil potential of immature source rocks, Peters and Cassa (1994) suggest TOC contents: between 1 and 2 wt% as indicative of good potential; between 2 and 4 wt% as very good potential, and greater than 4 wt% as excellent oil potential (*c.f.* Langford and Blanc-Valleron, 1990; Jarvie, 1991; Dembicki, 2009). In our study, samples that yielded TOC contents lower that 1 wt% were discarded.

Besides TOC, other geochemical parameters (S1, S2, S3, T_{max}, HI, OI, GP, and PI) were considered in our interpretations (Tables 1 and 2), as maturity is another aspect to be analyzed when evaluating oil and gas generation. According to Peters and Cassa (1994), TOC >2.0 wt% and S2 >10.0 indicate that the source rocks are rich in organic matter. Hydrogen index (HI) values exceeding 200 mg HC/g TOC indicate the oil-producing potential of the organic matter, whereas T_{max} greater than the reference temperature of 430 °C (Tissot et al., 1987) is an indication that the organic matter is starting the maturation stage for hydrocarbon production.

4.1. The middle shelf

To represent the middle shelf, 660 core samples were selected from seven exploratory wells (Fig. 1C). As mentioned above, only samples yielding TOC contents close to or higher than 1 wt% were considered in the analysis. Thus, out of 156 samples representative of the Mundaú Formation, only 136 (87%) yielded acceptable TOC contents; out of 357 samples representative of the Paracuru Formation, 297 (83%); out of 41 samples representative of the Uruburetama Member, 29 (71%), and out of 106 samples representative of the Itapajé Member, only 31 (29%) were used in the analysis.

4.1.1. Source-rock geochemistry

TOC contents varied according to the stratigraphic unit of the middle shelf (Table 1). High TOC contents are observed in the Mundaú and Paracuru formations (Fig. 3). The Paracuru Formation is the most promising because TOC contents indicate good, very good, or excellent oil-generating potential. The Uruburetama and Itapajé members of the Ubarana Formation yield low TOC contents and are predominantly classified as of poor and fair potential, and secondarily as of good potential (Fig. 3C).

All the stratigraphic units yielded low S1 values (Table 1). Additionally, the S1 vs. TOC diagram (Fig. 3A) suggests a massive presence of indigenous hydrocarbons, where free hydrocarbons (S1) are possibly a result of degradation and in situ thermal cracking of organic matter or expelled oil (Hunt, 1995). However, high S1 values contrasting with low TOC contents, as observed for seven samples of the Paracuru Formation, is an indication of a contaminated origin (Fig. 3A).

The S2 vs. TOC diagram (Fig. 3B) suggests that the potential to generate oil is low for most of the stratigraphic units of the middle shelf, excepting the Paracuru Formation. The high degree of organic matter preservation is indicated by the high TOC and S2 values observed for the Paracuru Formation. Additionally, the results for this unit are divided into two trends (Fig. 3B). In the first trend, S2 and HI values increase as TOC contents also increase (parallel direction to the HI = 600 boundary – Fig. 3B). In the second trend, high S2 and HI values but low TOC contents are observed (samples parallel to y-axis – Fig. 3B). A positive indication for oil and gas generation and fair to very good potential is suggested for the first trend (Fig. 3B and C).

Rock-Eval pyrolysis results show a nearly linear correlation of S1 and S2 with TOC contents for the middle shelf (Fig. 3C). The predominant Mundaú and Paracuru formations exhibit the best (highest quality) source rocks, of excellent or good oil-generating potential (Fig. 3C). On the other hand, the Uruburetama and Itapajé members stand opposite to those formations (Fig. 3C). For both members, the generating potential and quality of source rocks are poor or fair. The HI values indicate a predominance of gas and oil prone source rocks for the Paracuru Formation, classifying them as good or excellent (Fig. 3D). The Mundaú Formation is less promising when compared to the Paracuru Formation, as indicated by the lower HI and TOC contents. The Uruburetama and Itapajé members are predominantly oil and gas prone (Fig. 3D).

4.1.2. Organic matter type

The organic matter of the Mundaú Formation is predominantly of type III, with a minor presence of type II (Fig. 4A). Additionally, it is possible to infer from the Van Krevelen diagram that kerogen is of type III, probably derived from strongly degraded terrestrial or algal organic matter (Horsfield et al., 1994) (Fig. 4B). The HI vs. T_{max} diagram also indicates the predominance of type-III organic matter. Moreover, oil-prone source rocks are indicated by TOC contents >1 wt% and HI > 350, whereas gas potential is indicated by TOC contents >0.5 wt% and HI > 150 (Hunt, 1995). Regarding the Mundaú Formation, these parameters indicate oil and mainly gas-prone kerogen (Fig. 4B).

Kerogen types II and III with a minor contribution of kerogen type I characterize the Paracuru Formation in the middle shelf (Fig. 4A). As shown in the Van Krevelen diagram, kerogen type II is mainly derived from algal (phytoplankton) organic matter (Fig. 4B). The diversity of results regarding kerogen types attest the interpretations of a transitional environment (lacustrine, marine, and terrestrial) for the Paracuru

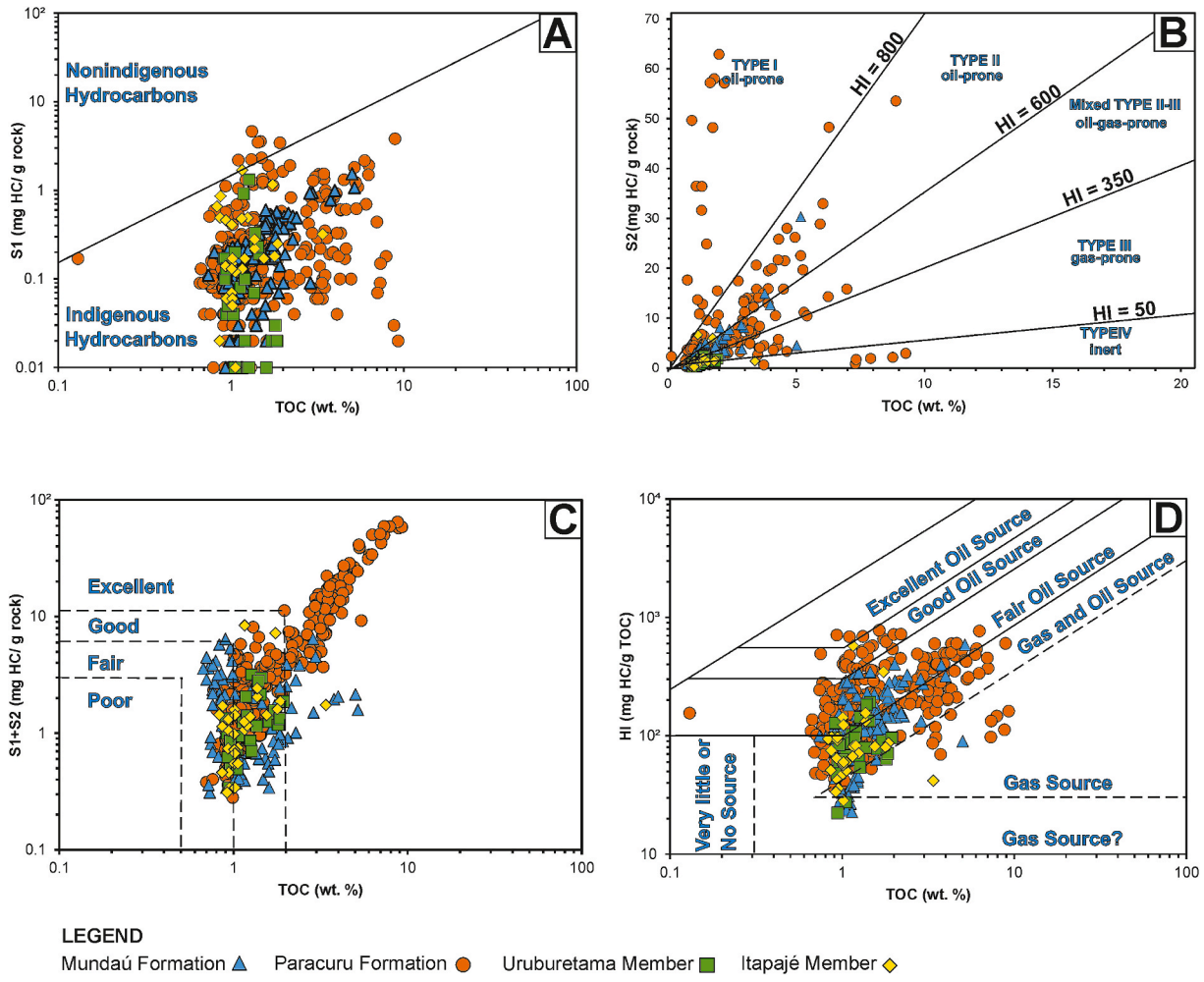

Fig. 3. Characterization of the source rocks sampled by well drillings located in the middle shelf of the Mundaú sub-basin. A) Amount of free hydrocarbons present in the organic matter (S1) versus organic carbon content (TOC). B) Amount of hydrocarbons generated by thermal cracking (S2) vs. TOC, indicating kerogen quality and kerogen types. C) Genetic potential (S1+S2) vs. TOC, indicating oil generating potential. D) Hydrogen index (HI) vs. TOC, indicating oil and gas potentials.

Formation. Mixed kerogen types are typical of environments receiving contributions from continental and marginal marine organic matter, able to generate oil and gas accumulations. Furthermore, the corresponding low OI and high HI values represented in the HI vs. OI diagram indicate good preservation of the organic matter during and after the deposition of the sediments (Fig. 4A). The HI vs. T_{max} diagram also suggests kerogen type II and III, and that the Paracuru Formation is mainly oil prone and subordinately gas prone (Fig. 4B).

Nevertheless, two populations are distinguished. The first one is marked by HI < 300 mg HC/g TOC and a negative correlation with T_{max}. This population (Fig. 4B) is related to the first trend observed in the S2 vs. TOC diagram (Fig. 3B) and probably represents the best source rocks. The second population yields HI ranging from 400 to 800 mg HC/g TOC, corresponding to T_{max} <425 °C (Fig. 4B), and is related to the second trend observed in the S2 vs. TOC diagram (Fig. 3B). The integration of these results, namely low TOC and T_{max}, high HI, and mixing and variations of kerogen types, signals that the second population of the Paracuru Formation is less promising regarding the generation of oil.

The (low) HI and OI values corresponding to the Uruburetama and Itapajé members point to the predominance of kerogen types IV and III (Fig. 4A). The HI vs. T_{max} diagram (Fig. 4B) indicates a predominantly inert kerogen, but with the potential to generate gas. Thus, the combined source-rock and organic-matter geochemistry indicates that the Uruburetama and Itapajé members of the Ubarana Formation are the least promising oil source rocks.

4.1.3. *Thermal maturity*

The degree of maturity was based on the vitrinite reflectance (Ro_{calc}), T_{max} values, production index (PI) and the Van Krevelen diagram. These indexes are usually used to evaluate source-rock and oil window. The Van Krevelen diagram indicates that the Mundaú Formation source rocks are thermally mature (Figs. 4B and 5B). In the PI vs. T_{max} diagram, most of the samples fall in the oil or early oil zone (Fig. 5A). This result is also supported by the Van Krevelen diagram that shows Mundaú samples in the oil generation window (Fig. 4B). Regarding the depth, the deeper the burial, the higher the T_{max} values and the potential of generating light oil and gas (Fig. 5B).

Similarly to the Mundaú Formation, the thermal maturity of the Paracuru Formation is controlled by its burial history, reaching the maturity required for oil generation (Fig. 5B). The Van Krevelen diagram indicates that the Paracuru Formation source rocks are immature to over mature (Fig. 4B). The T_{max} vs. depth diagram discriminates two groups of samples – one preferentially falling in the oil generation window (ranging from the oil window to the gas zone, with depths greater than 2500 m), and the other falling in the immature zone, close to the oil window (depths between 2500 m and 1000 m approximately) (Fig. 5B). These two groups comprise the trends discussed in sub-item 4.1.1 and the populations discussed in sub-item 4.1.2 (Figs. 3B, 4B and 5B).

The samples of both Uruburetama and Itapajé members of the Ubarana Formation indicate either immature or in the early oil zone

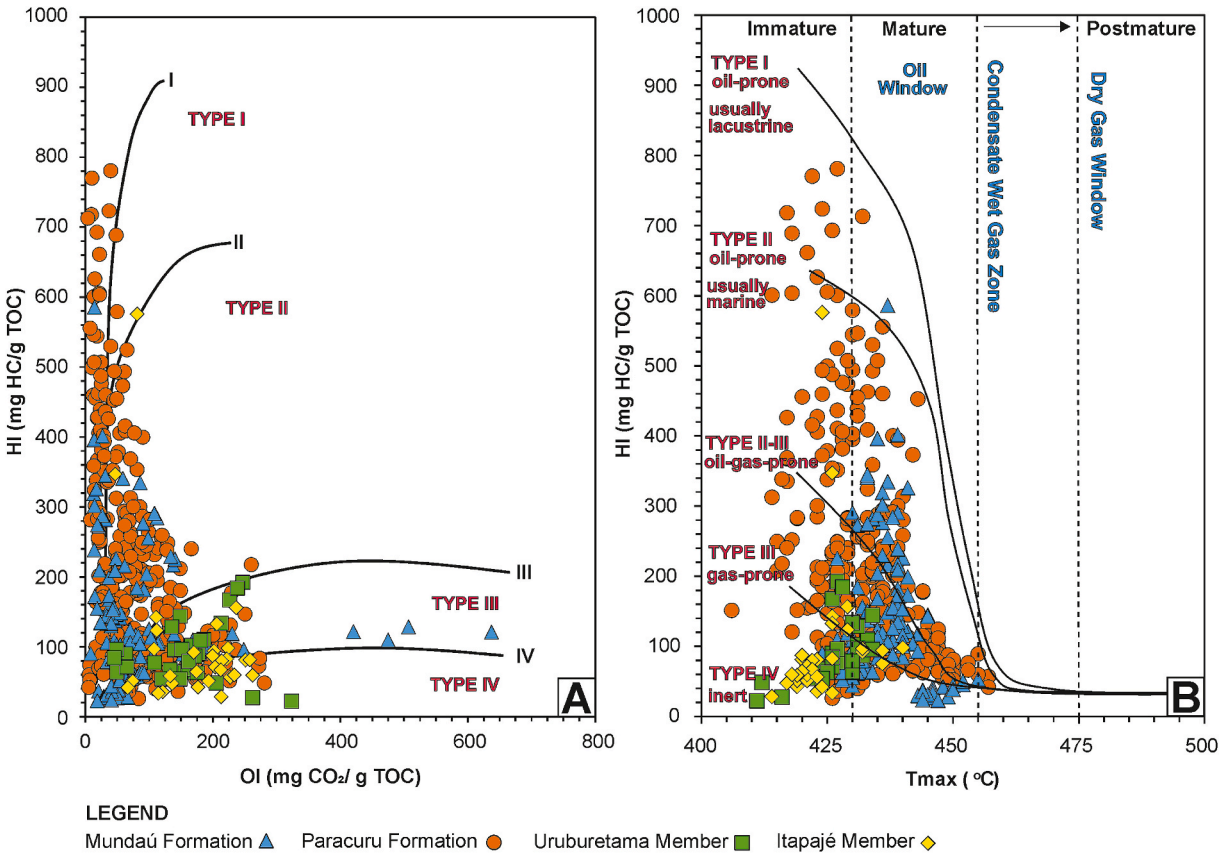

Fig. 4. Types of kerogen and thermal maturity characterization of the source rocks sampled by well drillings located in the middle shelf of the Mundaú sub-basin. A) Hydrogen index (HI) versus oxygen index (OI), and B) HI versus temperature at the peak of thermal cracking (T_{max}) (modified after Hart and Steen, 2015).

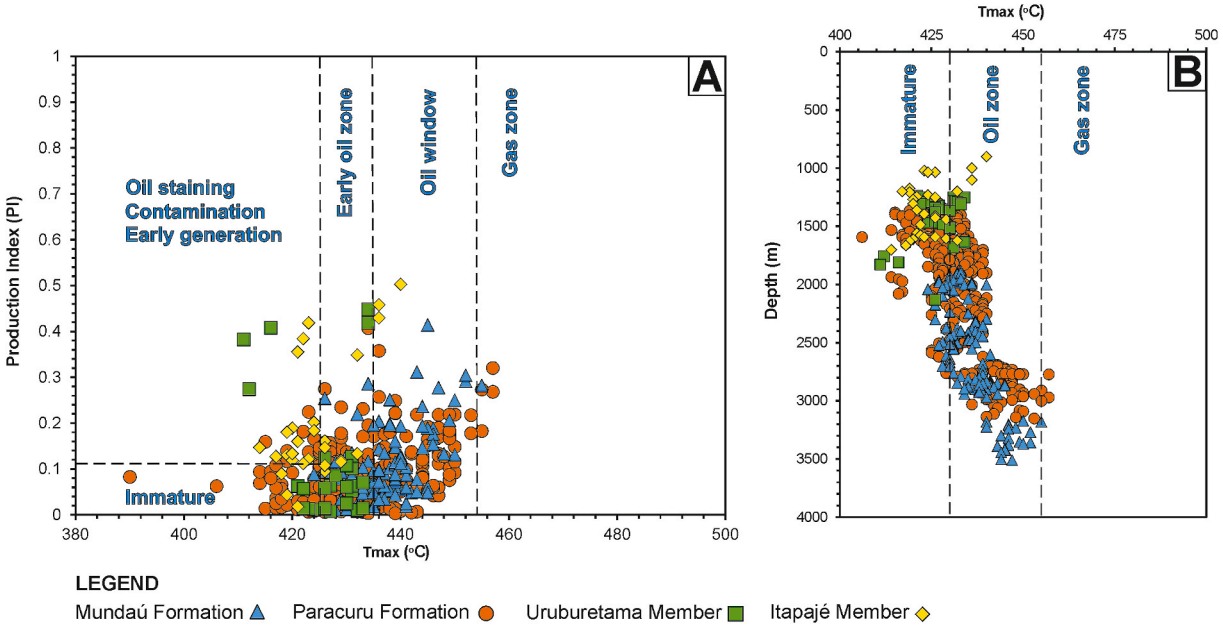

Fig. 5. Thermal maturity characterization of the source rocks sampled by well drillings located in the middle shelf of the Mundaú sub-basin. A) Production index (PI) vs. temperature at the peak of thermal cracking (T_{max}). (Modified after Peters, 1986 and Waples, 1994). B) Depth vs. T_{max}, indicating oil and gas generating potential.

(Figs. 4B, 5A and 5B). All samples from the Uruburetama and Itapajé members fall below the oil generation window of the PI vs. T_{max} diagram (Fig. 5) and there is no clear relationship between thermal maturity and burial depth. Therefore, the level of thermal maturity of the Ubarana Formation source rocks ranges from the immature to the early oil zone, with potential for incipient oil generation.

4.1.4. Hydrocarbon expulsion

Vitrinite reflectance (Ro_{calc}) points to a continuous increase in vitrinite macerals with depth (until 3500 m). Likewise, there is a gradual

increase in the relative hydrocarbon potential (RHP) until 1635 m (Fig. 6B), and then a constant decrease until 3500 m (Fig. 6B). The ASDL for the middle shelf is below the mark of 3500 m, while the hydrocarbon expulsion threshold is 1635 m. These results are positive perspectives regarding oil exploration in the Mundaú sub-basin.

The link between Ro_{calc} vs. depth and hydrocarbon expulsion threshold indicates that the mature source rocks correspond to the oil window, yielding Ro_{calc} values above 0.5%. These values are related to the predominance of the Mundaú and Paracuru formations on the middle shelf. This interpretation is also supported by T_{max} (Fig. 5A and B). Hydrocarbons that were generated were retained in the source rocks until the expulsion threshold was reached. Once the threshold was attained, the capacity of the source rocks to retain hydrocarbons gradually decreased (Fig. 6B).

4.2. The outer shelf

A total of 911 samples were selected from eight exploratory wells for the evaluation of the outer shelf (Fig. 1C). Applying the same criteria of data selection used for the middle shelf, out of 68 samples representative of the Mundaú Formation, 57 (83.8%) were used in this analysis; of out 406 samples representative of the Paracuru Formation 338 (83.2%); out of 158 samples representative of the Uruburetama Member, 132 (83.5%), and out of 279 samples representative of the Itapajé Member, 250 (89.6%) were used in this analysis, as listed in Table 2. When compared to the same units of the middle shelf, the formations and members of the outer-shelf yielded higher percentages of samples with TOC >1 wt%.

4.2.1. Source-rock geochemistry

In the outer-shelf, an increase in TOC contents is observed for all units, when compared to those of the corresponding ones in the middle shelf. For the Mundaú Formation source rocks, the potential varying from fair to excellent. Comparatively higher TOC contents indicate preferentially good to the excellent potential for the Paracuru Formation source rocks. The values for the Uruburetama and Itapajé members of the Ubarana Formation indicate fair and excellent potential, contrasting with the weaker results observed for these members on the middle shelf. The Paracuru Formation source rocks of the outer shelf yield the highest TOC contents of the study area.

The S1 vs. TOC diagram enables the identification of contamination and staining (Fig. 7A), confirming the presence of indigenous hydrocarbon in the Atum field, which is also indicated by the relatively low S1 and high TOC contents. These results also suggest that an indigenous source is related to areas not contaminated by migrated hydrocarbon. The correlation between S2 and TOC (Fig. 7B) provides an overall evaluation of some features, such as source-rock potential, HI range, and kerogen type. Thus, a fair potential is indicated for the Mundaú Formation; a fair to very good potential for the Paracuru Formation, and a fair to good potential for the Uruburetama and Itapajé members.

Additionally, S2 values show that, although the Paracuru Formation is the most promising when compared to the other units, the Uruburetama Member yields a higher mean S2 value. These results indicate the best potential of the Paracuru Formation and the Uruburetama Member source rocks in the Atum field. In general, as S2 increases, TOC also increases (Fig. 7B). This relationship indicates the evolution from a non-source to very good source potential, from the Mundaú Formation, Itapajé Member, Uruburetama Member to the Paracuru Formation.

The relationship between genetic potential (S1 + S2) and TOC

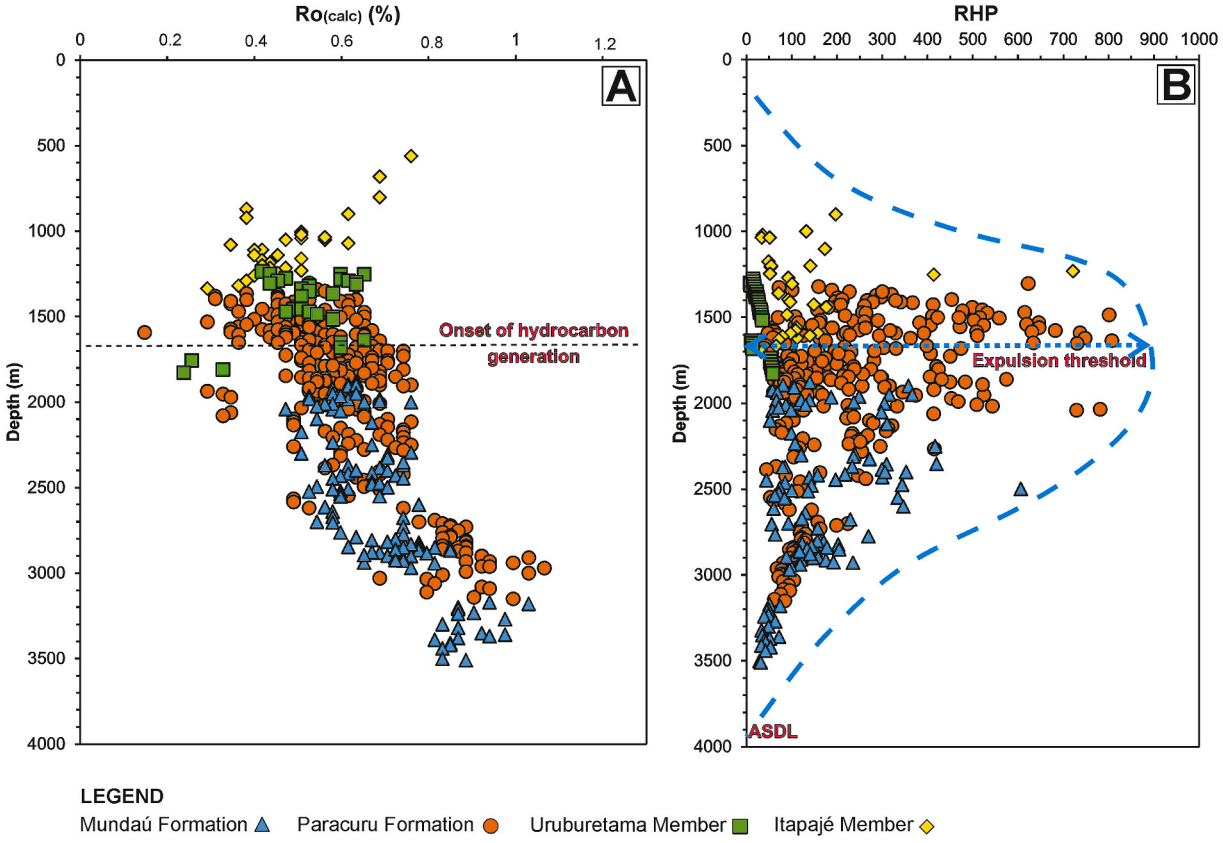

Fig. 6. Hydrocarbon generation and expulsion characteristics of the source rocks sampled by well drillings located in the middle shelf of the Mundaú sub-basin. A) Calculated vitrinite reflectance (Ro_{calc}) vs. burial depth. B) Relative hydrocarbon potential (RHP = [S1+S2]/TOC) vs. burial depth, and the indication of the hydrocarbon expulsion threshold and active source rock depth limit (ASDL) (Modified after Pang et al., 2019). The interception of the blue dashed line with the vertical axis determines ASDL. (For interpretation of the references to color in this figure legend, the reader is referred to the Web version of this article.)

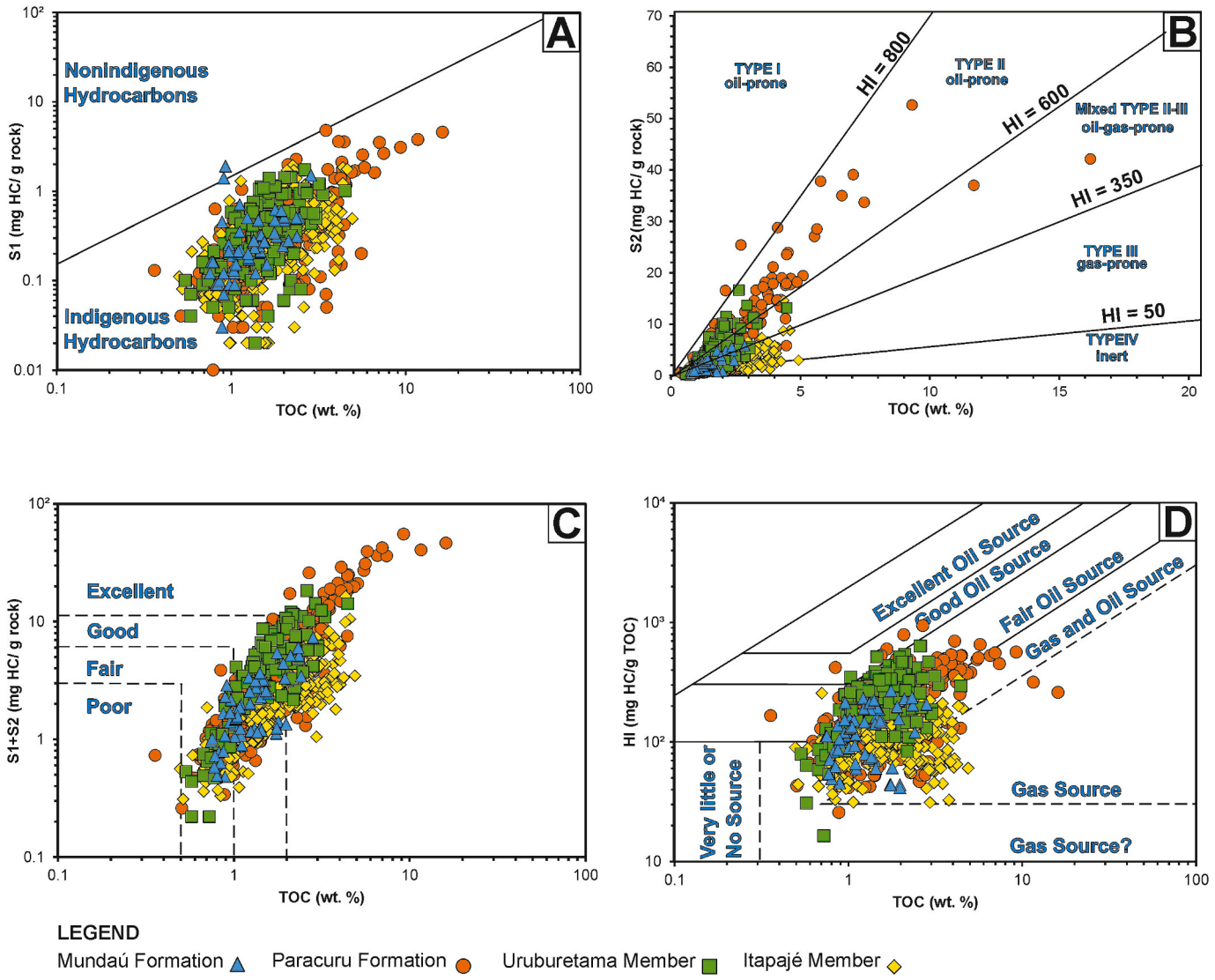

Fig. 7. Characterization of the source rocks sampled by well drillings located in the outer shelf of the Mundaú sub-basin. A) Amount of free hydrocarbons present in the organic matter (S1) versus organic carbon content (TOC). B) Amount of hydrocarbons generated by thermal cracking (S2) vs. TOC, indicating kerogen quality and kerogen types. C) Genetic potential (S1+S2) vs. TOC, indicating oil generating potential. D) Hydrogen index (HI) vs. TOC, indicating oil and gas potentials.

(Fig. 7C) indicates a fair to good source-rock potential for the Mundaú Formation; good and mainly excellent potential for the Paracuru Formation; fair to the excellent potential for the Uruburetama Member, and good to the excellent potential for the Itapajé Member (Fig. 7C). The HI vs. TOC diagram (Fig. 7D) attests the results for the Mundaú Formation, indicating a fair potential for oil generation and excellent potential for gas generation. A significant potential for oil generation and secondarily for gas generation is indicated for the Paracuru Formation. A fair potential for oil generation is indicated for the Uruburetama Member, while a higher potential for gas and oil generation is indicated for the Itapajé Member (Fig. 7D).

4.2.2. *Organic matter type*

The Van Krevelen diagram indicates kerogen type II and mainly type III (terrestrial organic matter) for the Mundaú Formation (Fig. 8A). In the HI vs. T_{max} diagram, the predominance of kerogen type III is attested, plus the indication of mixing of types III and II. The Mundaú Formation is gas prone, with a few samples plotting in the condensate wet gas zone of Fig. 8B. There is a considerable variation in the Paracuru Formation, with samples falling in practically all fields of Fig. 8A and B. In the HI vs. T_{max} diagram (Fig. 8B), a predominance of types II/III, III, and II is observed, followed by types I and IV and reflecting a wide mixing of organic matter types. This mixing is characteristic of transitional environments, such as restricted marine, deltaic, and lacustrine depositional systems (e.g., Condé et al., 2007). The oil generation potential expected for the Paracuru Formation is mainly within the oil window, even if a few samples plot in the condensate wet gas zone (Fig. 8B). Similarly to the Xaréu field, the wide predominance of oil-prone source rocks in the Paracuru Formation makes it a major source rock of the Ceará Basin.

4.2.3. *Thermal maturity*

The HI vs. T_{max} diagram indicates that the Mundaú Formation source rocks are mature to post-mature (Fig. 8B). It is possible to trace a maturity trend line on the PI vs. T_{max} and Depth vs. T_{max} diagrams (Fig. 9A and B) that increases as depth increases, as pointed out by the relationship between thermal maturity and burial depth. The source rocks of the Paracuru Formation are characterized as immature to post-mature (Fig. 8B), with predominance of samples falling in the oil window, which is also attested by the PI vs. T_{max} and Depth vs. T_{max} diagrams (Fig. 9A and B). Furthermore, the degree of depth is a relevant aspect for generations, such as see for Mundaú is related to Paracuru Formation.

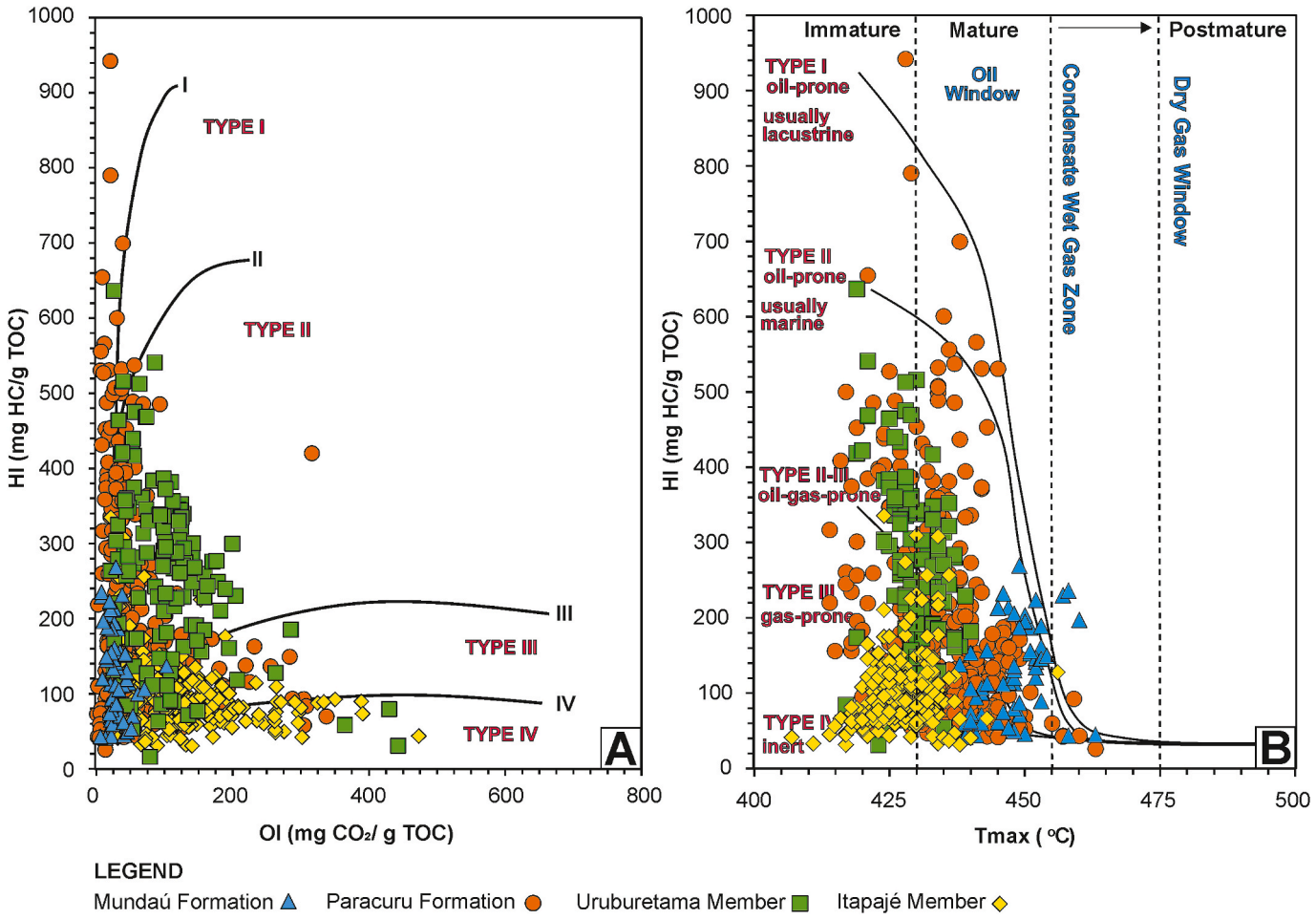

Fig. 8. Types of kerogen and thermal maturity characterization of the source rocks sampled by well drillings located in the outer shelf of the Mundaú sub-basin. A) Hydrogen index (HI) versus oxygen index (OI), and B) HI versus temperature at the peak of thermal cracking (T_{max}) (modified after Hart and Steen, 2015).

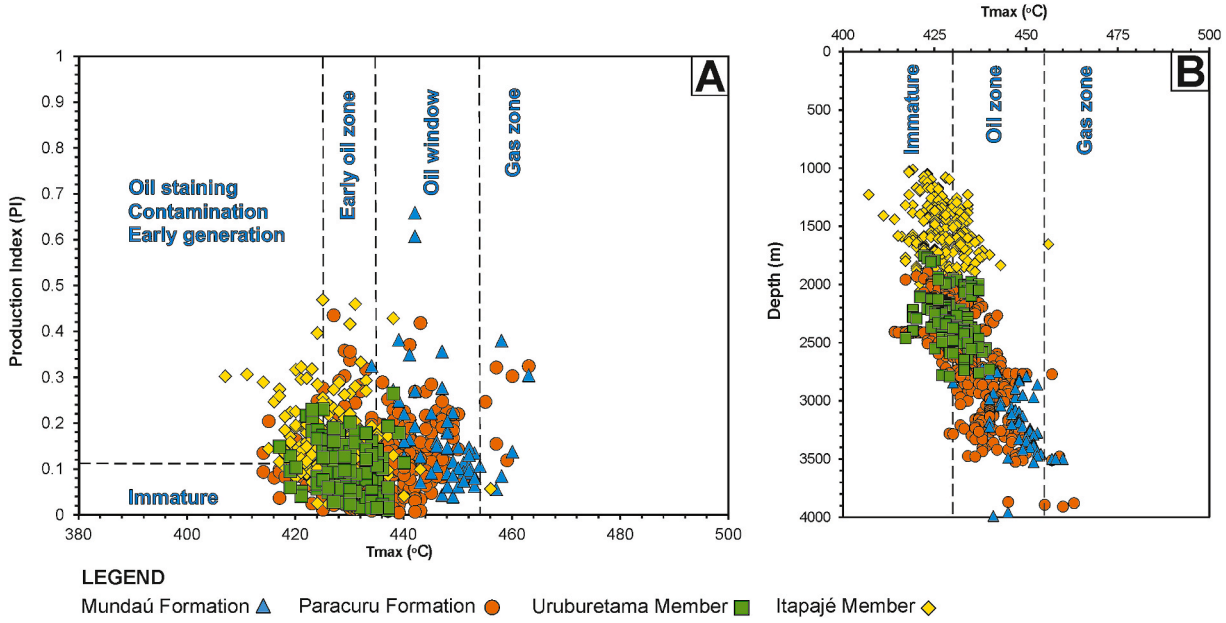

Fig. 9. Thermal maturity characterization of the source rocks sampled by well drillings located in the outer shelf of the Mundaú sub-basin. A) Production index (PI) vs. temperature at the peak of thermal cracking (T_{max}). (Modified after Peters, 1986 and Waples, 1994). B) Depth vs. T_{max}, indicating oil and gas generating potential.

The HI vs. T_{max} diagram indicates that the Uruburetama and Itapajé Member source rocks range from immature to mature (Fig. 8B). The results for the Uruburetama Member are better because the samples plot predominantly in the oil zone or early oil zone, and the thermal maturity increases with depth (Fig. 9B). These results indicate that the Uruburetama Member in the outer shelf has reached the thermal maturity to be considered a potential source rock for oil. On the other hand, the Itapajé Member has not reached thermal maturity for hydrocarbon generation or is still in the early mature zone (Fig. 8B) and is classified as immature in the HI vs. T_{max} diagram. Besides, this member is the shallowest (Figs. 5B and 9B). A few samples of the Atum field in the outer shelf or distal region fall in the oil zone (Fig. 9B). This can be interpreted as the maturity path increasing from the Itapajé Member to the Uruburetama Member, the Paracuru Formation and to the Mundaú Formation.

4.2.4. Hydrocarbon expulsion

Vitrinite reflectance (Ro_{calc}) values for the Atum field source rocks are listed in Table 2. The results show that as Ro increases, RHP increases up to a threshold and then decreases (Fig. 10A and B). Ro values ranging from 0.5 to 0.8% correspond to the hydrocarbon expulsion threshold. When Ro is lower than 0.5%, the source rocks may be producing hydrocarbons, but they are not expelled. When Ro exceeds 0.8%, hydrocarbons are expelled from the source rocks and consequently RHP decreases. The comparison of Fig. 9A and B shows that the predominance of source rock samples in the oil window is related to the Mundaú and Paracuru formations. The same predominance is seen in Figs. 10A and B for the Atum field. Therefore, expulsion of hydrocarbons occurs in both Mundaú and Paracuru formations.

There are differences in the hydrocarbon expulsion threshold as a result of the differences of burial depths of source rocks in the shelf and in deep waters (Figs. 6B, 10B and 10C). The hydrocarbon expulsion threshold in the Atum Field is 2106 m (Fig. 10B), of the middle shelf is 1635 m (Fig. 6B), and of the deep-water source rocks is 3632 m (Fig. 10C). The source rocks occur between 561 m and 4080 m in oil fields of the shelf (Figs. 6B and 10B). These results corroborate the more effective process of burial in the shelf-break limit represented by the Atum Field and justify the more expressive thermal maturity. From the deep-water source-rock analysis, the source rocks occur between 2754 m and 5007 m (Fig. 10C). The Atum field exhibits ASDL below 4500 m, and for deep waters, this limit is close to 6000 m.

5. Distribution of the source rocks

5.1. Well-log correlations via transects

Source-rock intervals contain a mixed succession of genetically and stratigraphically associated organic-rich shale, mudstone, siltstone and/or carbonate layers occurring within distinct units. Four transects (Figs. 11 and 12) illustrate the geochemical behavior and corresponding facies association distributions. The majority of the source rocks of the Mundaú Formation are located in the middle shelf, as revealed by 1-CES-80, 1-CES-45A, 1-CES-08, 4-CES-13, and, in minor proportion, in the outer shelf (see wells 1-CES-44, 4-CE-12A e 1-CES-78). A geochemical pattern is defined by increasing TOC contents towards the top of the Mundaú Formation (Line 1 in Figs. 11 and 12). Mudstone is the lithology chiefly associated with TOC enrichment, with kerogen type III suggesting gas-prone characteristics.

As there is no great variability between geochemical parameters in the lower and middle sections of the Paracuru Formation, these were grouped, possibly indicating similar organic facies. Low hydrogen indexes (HI) appear to correlate with sandstone interlayered with mudstone or shale. Abrupt increases in the parameter values are observed close to the Trairí Member top layers (Line 2 in Figs. 11 and 12), matching, in some wells, with a lithological change between shales and carbonates. For example, and as seen in all well logs, TOC contents are relatively low in the lower member the Paracuru Formation, but increase upwards, reaching high values in the middle and upper members close to the top of the Trairí Member. Likewise, HI also increases. Despite the minimal contribution of plant material from the continent, the high HI values obtained at these levels were likely caused by organic matter derived from hydrogen-rich algal material, characterizing a predominant lacustrine environment. The overall high HI and RHP

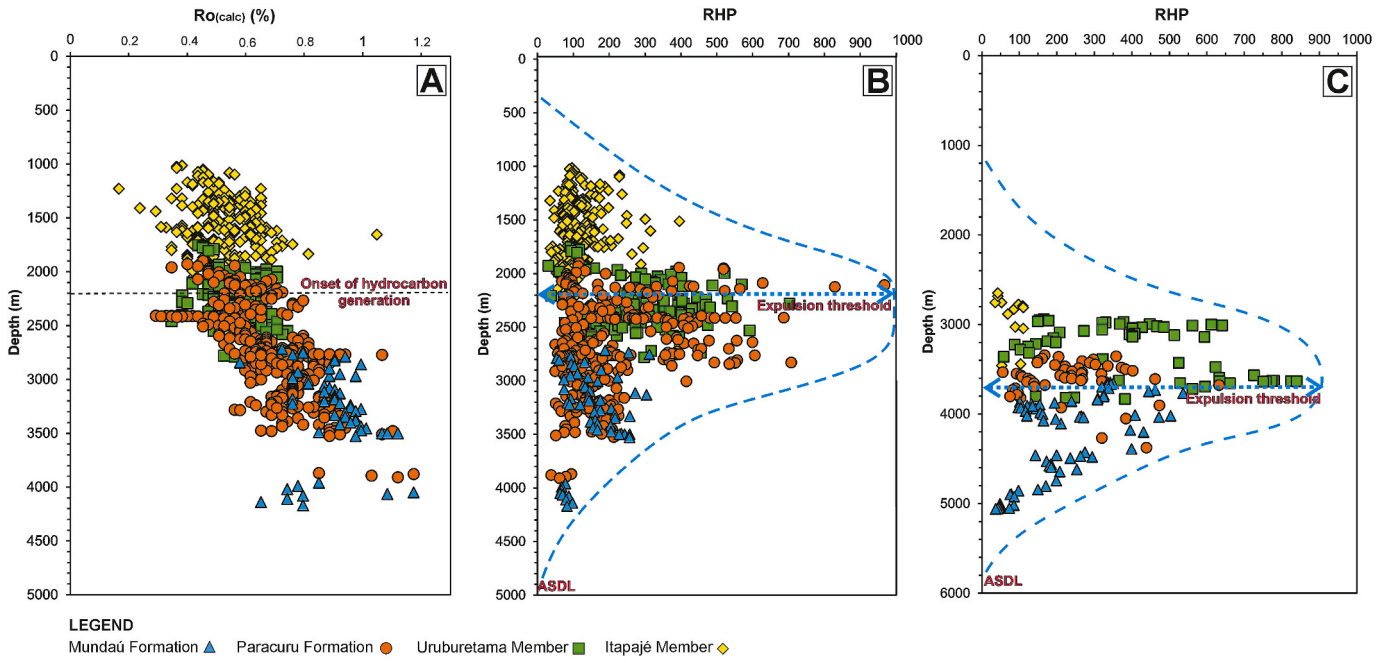

Fig. 10. Hydrocarbon generation and expulsion characteristics of the source rocks sampled by well drillings located in the outer shelf of the Mundaú sub-basin. A) Calculated vitrinite reflectance (Ro) vs. burial depth. B) Relative hydrocarbon potential (RHP = [S1+S2]/TOC) vs. burial depth, and the indication of the hydrocarbon expulsion threshold and active source rock depth limit (ASDL) (Modified after Pang et al., 2019). and C) Relative hydrocarbon potential (RHP = [S1+S2]/TOC) vs. burial depth, and the indication of the hydrocarbon expulsion threshold and active source rock depth limit (ASDL) for deep-water domain.

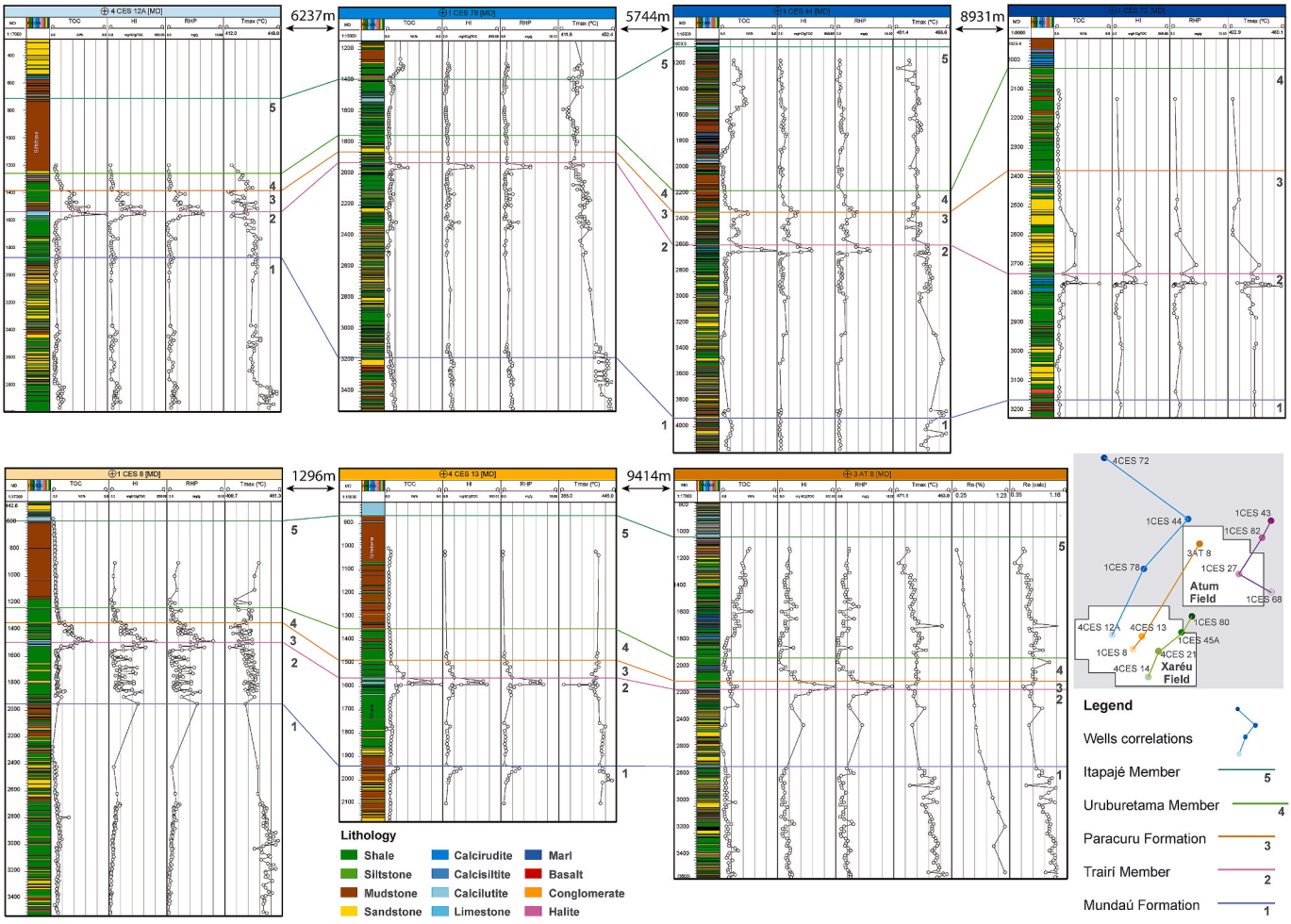

Fig. 11. Two transects, represented by the blue and orange lines in the schematic plan view (see also Fig. 1C). Well logs include stratigraphic columns and geochemical profiles of the total organic carbon (TOC), hydrogen index (HI), relative hydrocarbon potential (RHP), and temperature maxima (T_{max}). Numbered correlation lines represent the top layers of the Mundaú Formation (1), Trairí Member (2), Paracuru Formation (3), Uruburetama Member (4), and the Itapajé Member (5). (For interpretation of the references to color in this figure legend, the reader is referred to the Web version of this article.)

values indicate that these levels are mainly oil prone according to the guidelines proposed by Peters (1986) and Peters and Cassa (1994).

The interval between the tops of the Trairí Member (Line 2 in Figs. 11 and 12) and of the Paracuru Formation (Line 3 in Figs. 11 and 12) is organic-matter rich. It has been found in all types of sediments, but the predominant lithology is shale interlayered with carbonate layers. In this interval, TOC contents are lower than those of the top of the Trairí Member. However, this interval shows TOC contents higher than those for the basal part of the Paracuru Formation. This increase is seen in well logs 4-CES-12A, 1-CES-44, 4-CES-72, 4-CES-13, 1-CES-8, 1-CES-45A, 4-CES-21, 1-CES-80, 1-CES-82. These high TOC intervals suggest that the occurrence of the source rock is relatively widespread. A correlation between depositional environments and tectonic events indicates variations in water levels leading to flooding and in water depths resulting in deep to semi-deep organic-matter deposition during low tectonic activity.

The predominant facies of the Uruburetama Member are shales and mudstones intercalated with carbonate layers, as seen in well logs 1-CES-82, 4-CES-14, 1-CES-43, 1-CES-78 (Line 4 in Figs. 11 and 12). TOC contents are relatively low but increase with depth, possibly indicating better source rocks in deeper organic-matter burial intervals. Most of the shales yield TOC contents ˂1 wt%, which is the limit adopted in this study. From the outer shelf portion, there is a predominance of marine organic matter input. The source rock deposition, whereas low ratios TOC, indicate major planktonic and/or benthic algae input associated with marine environments.

Mudstone is the main facies of the Itapajé Member, which is sometimes interlayered with sandstone or shale (Line 5 in Figs. 11 and 12). A few core samples from wells drilled in the middle shelf yielded indexes indicative of hydrocarbon generation. The data previously presented shows highly reworked continent-derived sediments, perhaps in a highly oxic depositional environment with sandstone (wells 1-CES-80, 4-CES-21, 1-CES-45A, 4-CES-14). This variation could account for a higher terrigenous contribution and reworking during marine regression. The values of the TOC increase in the outer shelf (e.g., 1-CES-68, 1-CES-27, 1-CES-82, 1-CES- 43, and 1-CES-44).

5.2. *Well-log correlations via isoline maps*

The geochemical values from the Mundaú Formation are heterogeneously distributed on isoline maps (Fig. 13), which is in part due to the fact that the Mundaú Formation rift sequence has never been completely drilled and fault activities on the borders of the Mundaú sub-basin contribute to changes in sedimentation and thickness (Figs. 11 and 12). Minimum TOC contents (<0.5 to 1 wt%) are observed in the center of the field represented in purple in Fig. 13A. This field corresponds to regions of very low GP, also represented in purple in Fig. 13B, and to HI values lower than 100 mg HC/g TOC. As shown previously, the HI vs. OH and the HI vs. T_{max} diagrams indicate residual or inert organic carbon for the middle shelf and kerogen types IV and III for the outer

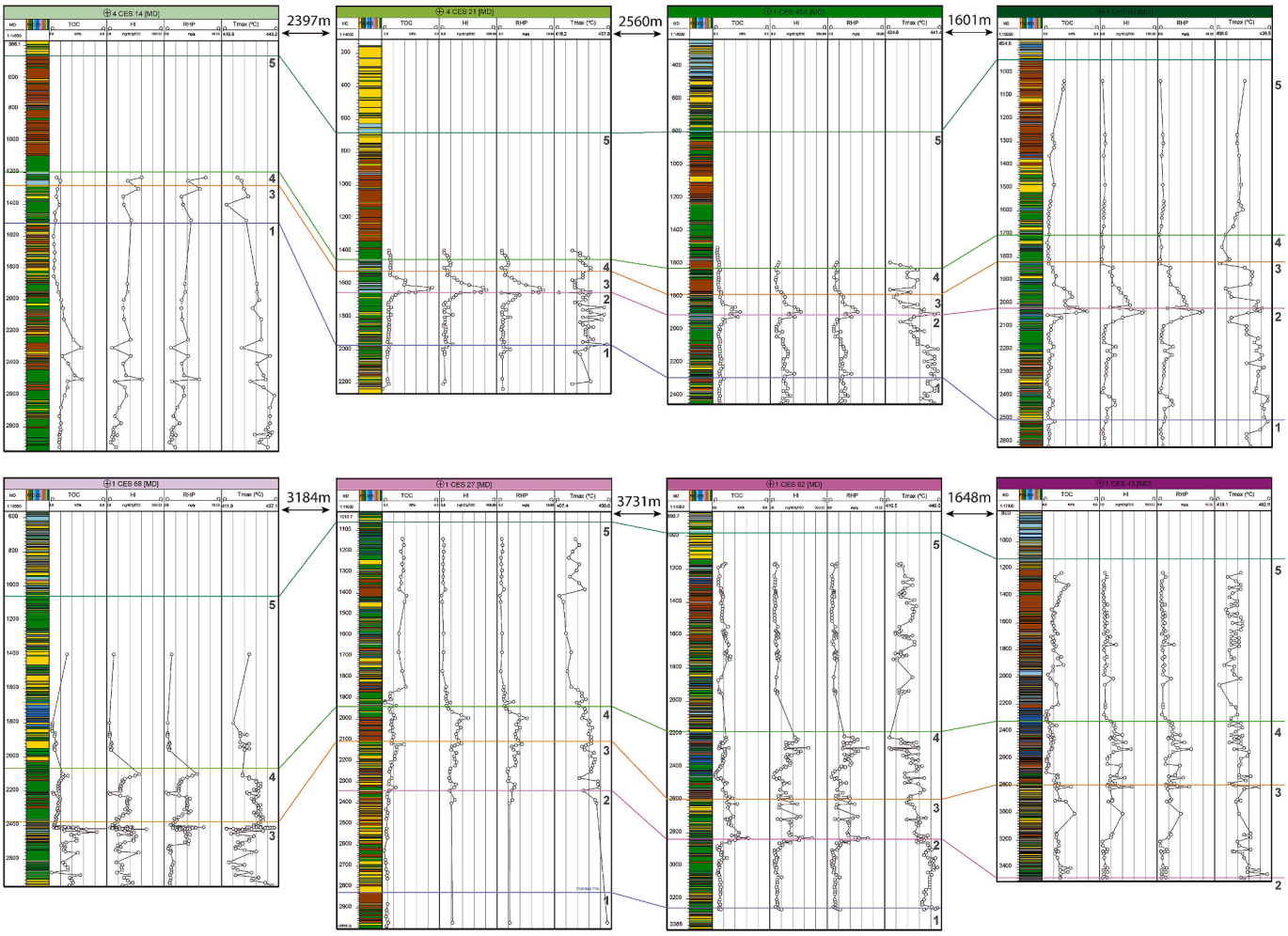

Fig. 12. Two transects represented by the green and purple lines in the schematic plan view of Fig. 11 (see also Fig. 1C). Well logs include stratigraphic columns and geochemical profiles of the total organic carbon (TOC), hydrogen index (HI), relative hydrocarbon potential (RHP), and temperature maxima (T_{max}). Numbered correlation lines represent the top layers of the Mundaú Formation (1), Trairí Member (2), Paracuru Formation (3), Uruburetama Member (4), and the Itapajé Member (5). (For interpretation of the references to color in this figure legend, the reader is referred to the Web version of this article.)

shelf (Figs. 4 and 8, respectively). These datasets suggest highly oxidized terrestrial organic matter for the Mundaú Formation in the central region of Fig. 13A. Regarding T_{max} in the central area of the Atum field, there is a set of T_{max} >450 °C that extends outwards in an E-W trend (orange zone in Fig. 13D). Other parameters decrease along with this E-W trend, such as TOC, GP and HI (blue and green zones in Fig. 13A, B and 13C). This region lies underneath a thicker sedimentary package (e.g., well logs 1-CES-80, 1-CES-82, and 4-CES-13 in Figs. 11 and 12). This region responds for oil and mainly gas generation (Figs. 4, 5, 8 and 9). These results are in agreement with the sample arrangement of the outer shelf, which is mainly distributed in the gas zone.

The best source rocks of the Mundaú Formation are related to a small area close to well 4-CES-14 in the middle shelf (signaled in red and yellow in Fig. 13A–C) and the pale green area in Fig. 13D. TOC contents >2.5 wt% are recorded for these areas. The fact that these rocks were initially rich in organic matter suggests that good preservation conditions were established during the deposition of the Mundaú Formation sediments. Besides the relatively high TOC contents, HI values are also high and GP increases with TOC. There is a decrease in T_{max} values, which reach good values for oil generation (<450 °C). The small area signaled in red and yellow in Fig. 13A–C is stretched along the NW-SE direction, which is parallel to the Mundaú Fault (Fig. 1C). The best area for source rock generation is related to wells*1-CES-43 e 1-CES-82*, located close to the slope. This area (green in Fig. 13A) is suggestive of the continental contribution in this segment.

The preparation of the isoline maps of the Paracuru Formation was made combining the information on stratigraphic markers provided by ANP and geochemical data, which resulted, for interpretative purposes, in the subdivision of the Paracuru Formation into the lower and upper Paracuru formations. The lower Paracuru Formation (Fig. 14) groups a total of 132 core samples located at depths below the top of the Trairí Member (line 2 in Figs. 11 and 12) and above the top of the Mundaú Formation (line 1 in Figs. 11 and 12). The upper Paracuru Formation (Fig. 15) includes a total of 503 core samples located at depths below the top of the Paracuru Formation (line 3 in Figs. 11 and 12) and above the top of the Trairí Member (line 2 in Figs. 11 and 12).

Regarding the lower Paracuru Formation, the area closes to well 1-CES-27 and represented in purple in Fig. 14A corresponds to TOC contents <1 wt%. The area closes to well 3-AT-08 and represented in red in Fig. 14C corresponds to high HI values of up to 400 mg HC/g TOC. Both areas are defined in the outer shelf, close to the Atum Field, for which a geochemical correlation is observed between HI values and the occurrence of kerogen type I and mainly kerogen type II (Figs. 3B and 4B). This relationship indicates not only mixing of lacustrine and marine environments, but also conditions favorable to the deposition of halite and carbonates in the Trairí Member. These results, together with GP ≤ 5 mg HC/g rock (Fig. 14B), point to little potential of oil generation. The west side of the area close to well 1-CES-27 is characterized by low TOC

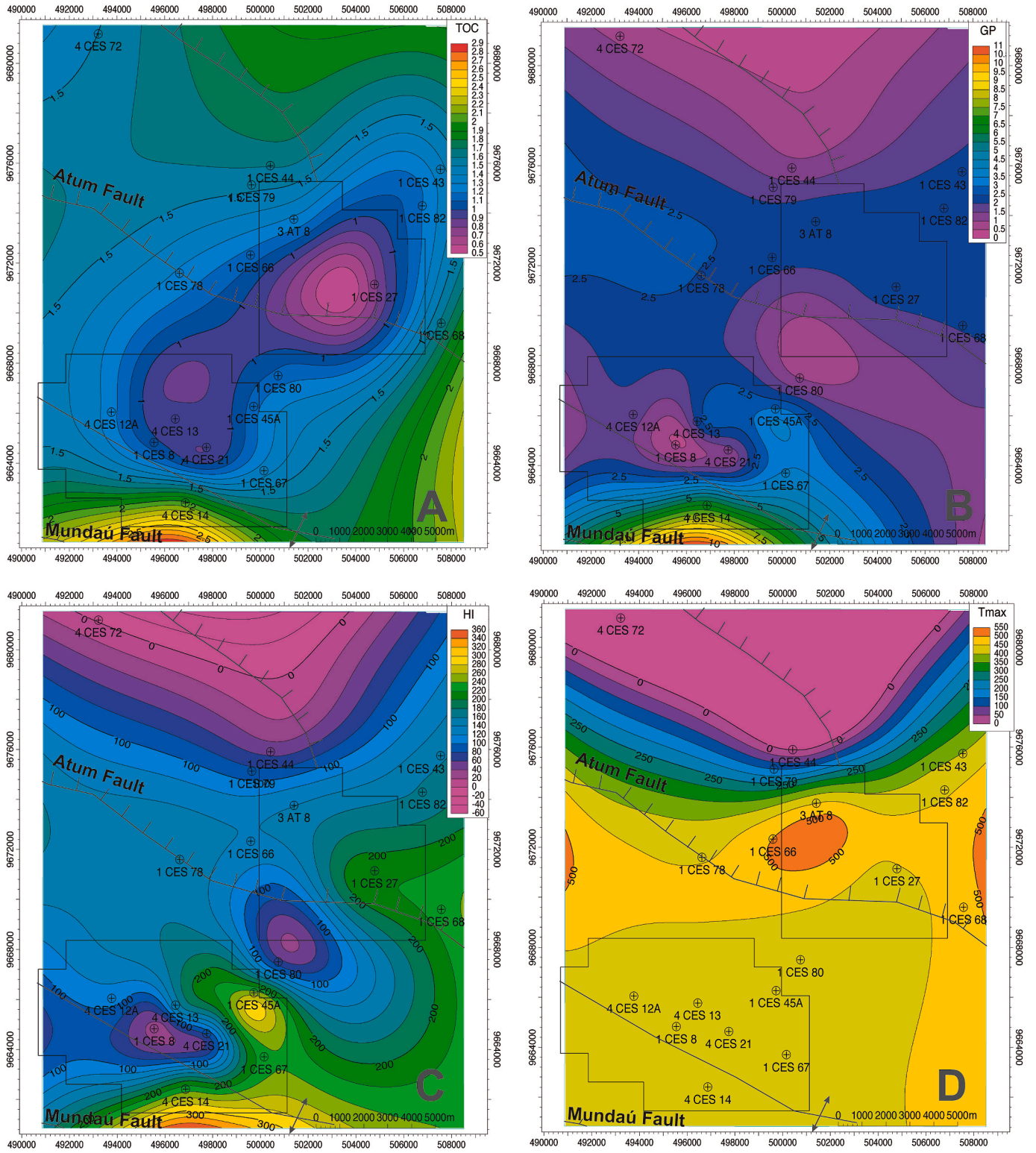

Fig. 13. Isoline maps for the characterization of the Mundaú Formation source rocks. A) Spatial distribution of mean TOC (wt. %) contents up to line 1 in Figs. 11 and 12. B) Genetic Potential (GP in mg HC/g rock). C) Hydrogen Index (HI in mg HC/g TOC). D) Temperatures at the peak of thermal cracking (T_{max} in °C). T_{max}, GP and HI were calculated using mean values of Rock-Eval pyrolysis parameters obtained for 175 samples (Tables 1 and 2).

contents (represented in dark blue in Fig. 14A), GP $\leq$ 2.5 mg HC/g rock (purple in Fig. 14B), and low HI values (purple in Fig. 14C), which indicates kerogen type IV. Both the Paracuru Formation and the Trairí Member reach their maximum thickness in this area.

The best source rocks of the lower Paracuru Formation are related to an E-W trend defined in the middle shelf by TOC contents >1.5 wt% (represented in green, yellow and red areas in Fig. 14A). GP values increase westwards (Fig. 14B) and HI values increase eastwards (Fig. 14C). HI values > 200 indicate kerogen types II and III, and are also interpreted as mixing between marine and terrestrial environments. The increase of HI values from E to W indicates higher contribution of marine kerogen type II in the middle shelf. On the other hand, high TOC (green

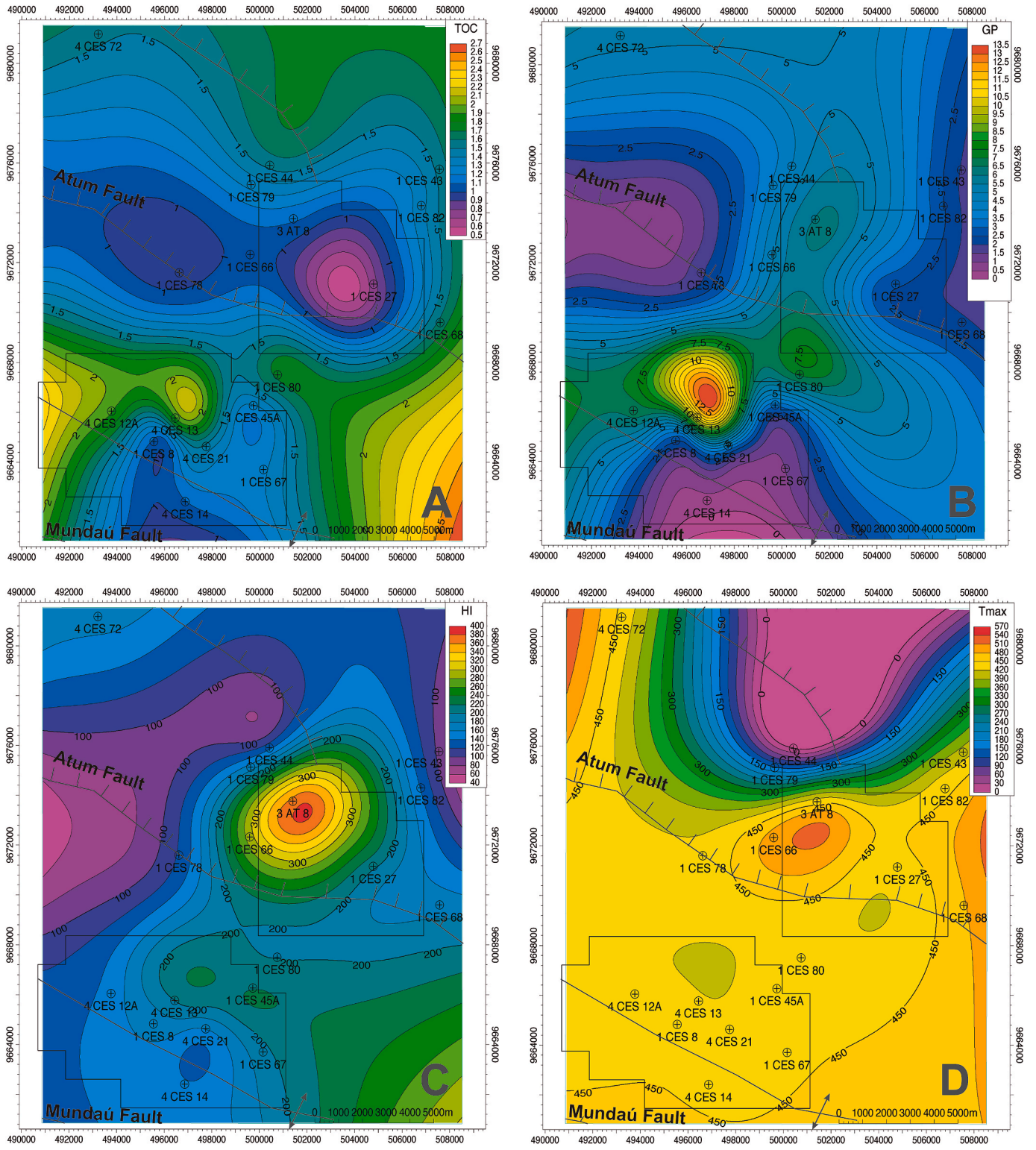

Fig. 14. Isoline maps for the characterization of the lower Paracuru Formation source rocks. A) Spatial distribution of mean TOC (wt. %) contents from line 1 to line 2 in Fig. 11 and 12. B) Genetic Potential (GP in mg HC/g rock). C) Hydrogen Index (HI in mg HC/g TOC). D) Temperatures at the peak of thermal cracking (T_{max} in °C). T_{max}, GP and HI were calculated using mean values of Rock-Eval pyrolysis parameters obtained for 132 samples.

and yellow areas in Fig. 14A) and low HI values (purple area in Fig. 14C) indicate significant terrestrial contribution; HI values close to 100 and 140 mg HC/g TOC correspond to kerogen type III. The T_{max} distribution in the lower Paracuru Formation is similar to that in the Mundaú Formation. The best source rocks (T_{max} <450 °C) correspond to the pale yellow and green areas in Fig. 14D, which are mostly located in the middle shelf and partially in the outer shelf. Higher T_{max} values (450–570 °C) are related to areas of little source rock potential within the outer shelf (Fig. 14D). These T_{max} values indicate gas-prone sources for the outer shelf.

Comparing the distribution of TOC isolines in the lower Paracuru Formation (Fig. 13A) with that of the Mundaú Formation (Fig. 14A), it is

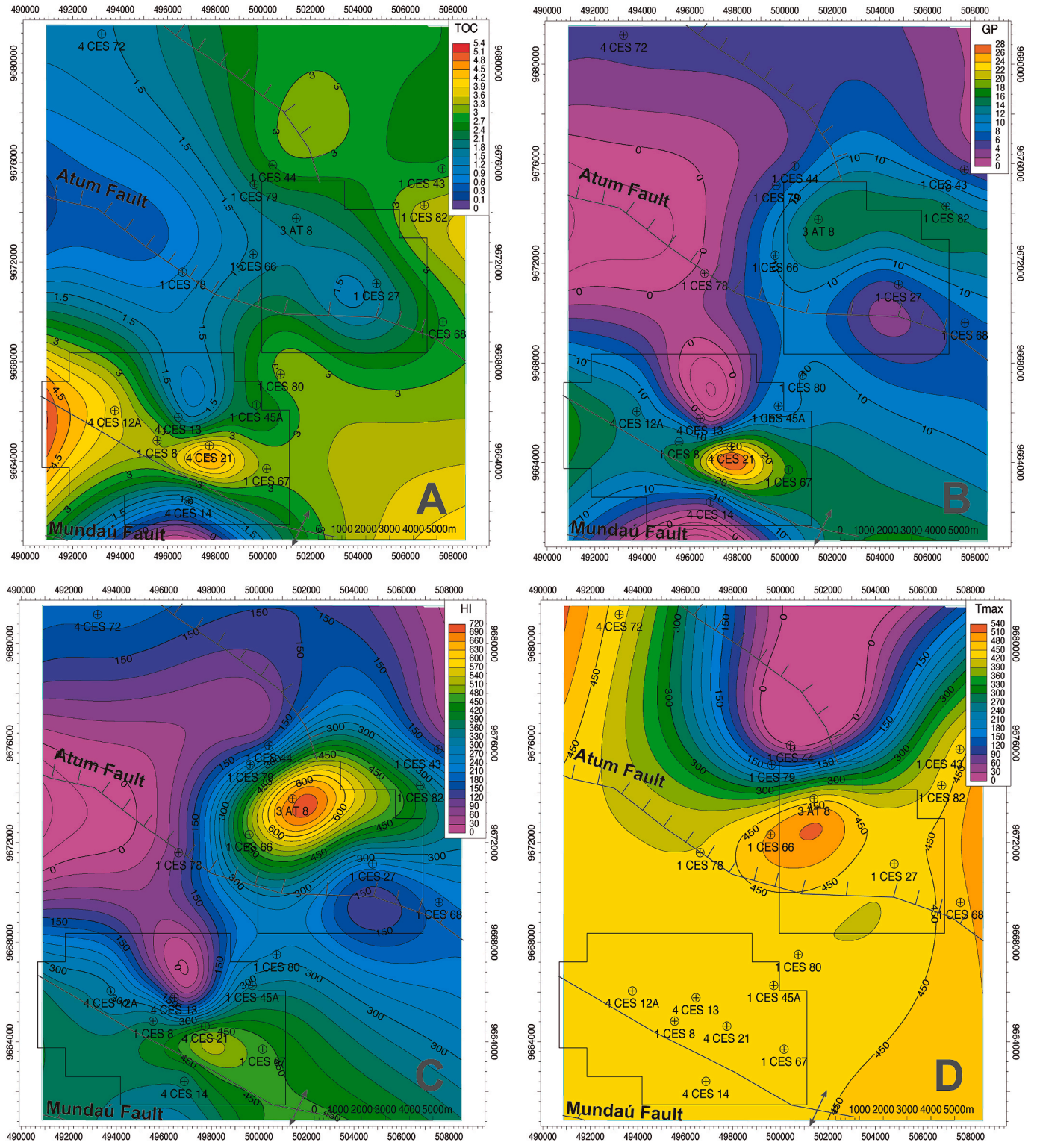

Fig. 15. Isoline maps for the characterization of the upper Paracuru Formation source rocks. A) Spatial distribution of mean TOC (wt. %) contents from line 2 to line 3 in Fig. 11 and 12. B) Genetic Potential (GP in mg HC/g rock). C) Hydrogen Index (HI in mg HC/g TOC). D) Temperatures at the peak of thermal cracking (T_{max} in °C). T_{max}, GP and HI were calculated using mean values of Rock-Eval pyrolysis parameters obtained for 503 samples.

possible to see a migration of low TOC contents basinward. The low TOC contents of the Mundaú Formation (represented in purple and blue in Fig. 13A) are located between the middle and outer shelves, whereas the low TOC contents on the Lower Paracuru Formation are located in a more distal position in the outer shelf (represented in purple and blue in Fig. 14A). The same is observed when it comes to higher TOC contents. The best source rocks of the Mundaú Formation were located in a more proximal position; these TOC isolines migrated to a more central position located in the middle shelf and corresponding to the lower Paracuru Formation (orange and yellow areas in Figs. 13A and 14A). These migrations are interpreted here as progradation.

An expansion of the higher TOC areas (compare Figs. 13A and 14A)

and an increase in TOC contents (Figs. 11 and 12) are observed in the lower Paracuru Formation, mainly in the middle shelf. These features suggest an increase in productivity or preservation (once TOC represents biogenic carbon). Decreases in TOC contents observed in the outer shelf suggest a decrease in source-rock quality and change of kerogen types towards the deeper parts of the basin. These results can be interpreted as a higher oil and gas potential for the middle shelf and gas potential for the outer shelf.

Contrasting geochemical data are observed in the upper Paracuru Formation, with TOC >1.5 wt% (Fig. 15A) and HI from 350 to 600 mg HC/g TOC (Fig. 15B). Kerogen type II is indicated for these source rocks (Figs. 3, 4, 7 and 8). In the outer shelf, located in a more distal area of the

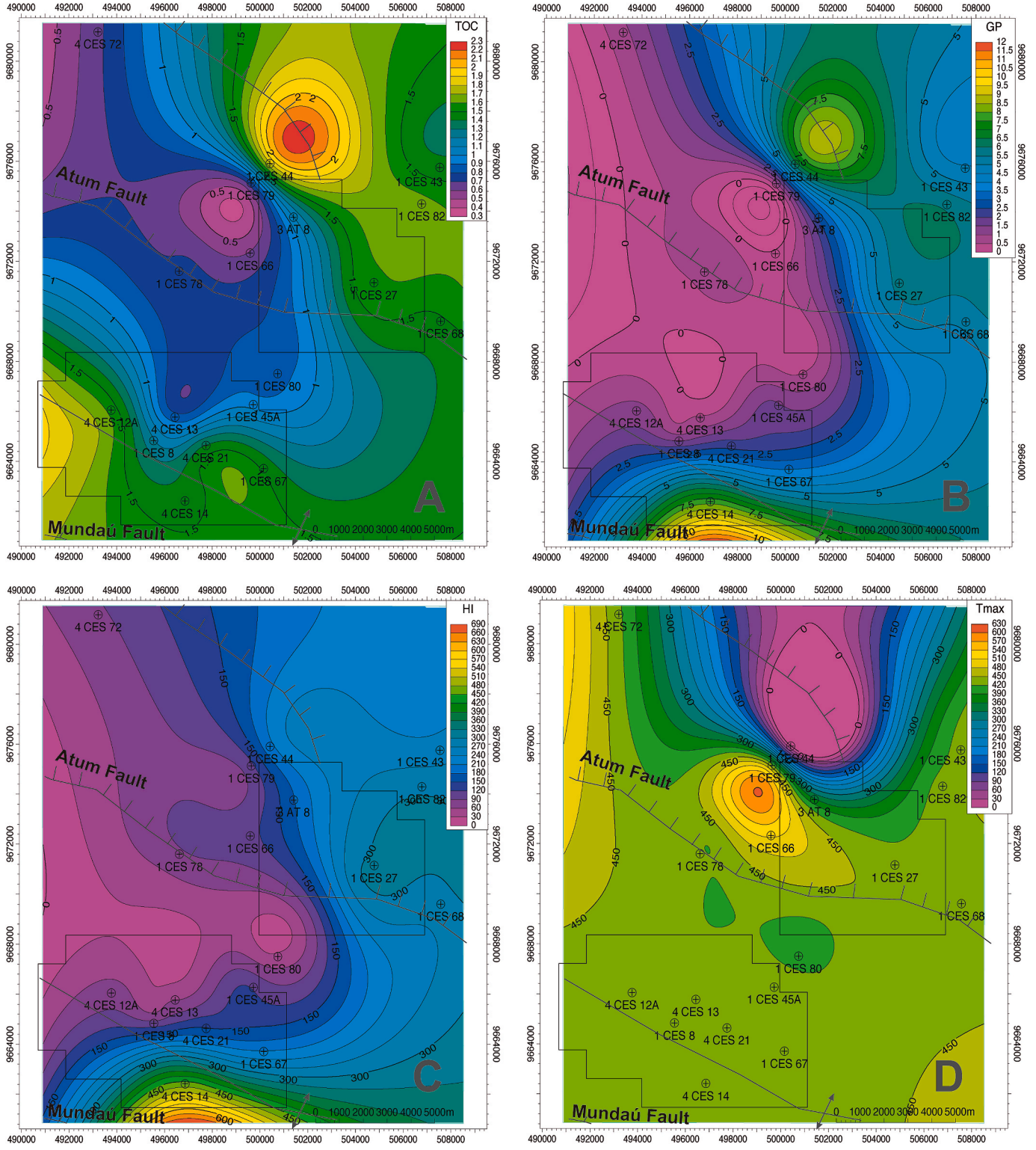

Fig. 16. Isoline maps for the characterization of the Uruburetama Member source rocks. A) Spatial distribution of mean TOC (wt. %) contents from line 3 to line 4 in Fig. 11 and 12. B) Genetic Potential (GP in mg HC/g rock). C) Hydrogen Index (HI in mg HC/g TOC). D) Temperatures at the peak of thermal cracking (T_{max} in °C). T_{max}, GP and HI were calculated using mean values of Rock-Eval pyrolysis parameters obtained for 161 samples (Tables 1 and 2).

Mundaú sub-basin, the signature of the upper Paracuru Formation is typically marine. This marine signature is the main feature that distinguishes the upper from the lower Paracuru formations in the outer shelf. In the middle shelf, slightly lower HI values (300–450 mg HC/g TOC) obtained for the upper Paracuru formation are interpreted as mixing of kerogen types II and III and terrestrial and marine contributions. The blue area in Fig. 15A representing TOC contents up to 1.5 wt% and the purple area in Fig. 15C representing HI values up to 150 mg HC/g TOC (kerogen type III) indicate continental paleo-environments.

The best source rocks of the upper Paracuru Formation, as indicated by the genetic potential (GP) isoline map, are represented by the green area in the outer shelf (top right of Fig. 15B) and red and orange areas in the middle shelf (bottom left of Fig. 15B). The green area is probably related to the generation of kerogen type II in the outer shelf (gas prone). The red and orange areas are related to mixed kerogen types II and III (gas and oil prone). Other areas showing good TOC contents are associated with low HI and low GP values.

The T_{max} isoline map of the upper Paracuru Formation (Fig. 15D) is similar to that of the lower Paracuru Formation. The most remarkable difference is related to the proximal areas in the middle shelf. The 450 °C isotherm of the lower Paracuru Formation is located in the southernmost part of the middle shelf (Fig. 14D). It is absent in the middle shelf, where T_{max} values do not exceed 400 °C (Fig. 14D). This result can be interpreted as a decrease in tectonic activity related to the transition between the post-rift and drift stages.

The organic geochemical data indicate very good conditions for hydrocarbon generation in areas with mean TOC contents from 1 to 4.5 wt% (represented in red, yellow, and green in Fig. 15A). A displacement of these areas towards the basin border is observed when Figs. 14A and 15A are compared. The landward migration is attested by higher parameter values, mainly TOC. This change in position is interpreted as retrogradation. Low values in the central position of the outer shelf are absent. This interval is characterized by a vast affected area, a more homogeneous range of values and landward facies migration.

The isoline maps of the Uruburetama Member of the Ubarana Formation display different patterns from those of the underlying formations and define three potential areas. The first is indicated by TOC isolines ranging from 1.5 to 2 wt% and is a distal area (represented in red in Fig. 16A). HI values are slightly lower than 300 mg HC/g TOC, pointing to kerogen types II and III. These features pointed to mixed marine and terrestrial contributions. A second promising area delimited by TOC isolines of 1.5 wt% (represented in green and yellow in Fig. 16A) is proximal to the southwestern portion of the middle shelf and can also be interpreted as of intermediate potential. Corresponding HI values range from 300 to 600 mg HC/g TOC (Fig. 16B) and indicate kerogen type II and marine signature. The third area is central, delimited by TOC isolines from 0.5 to 1 wt% (represented in purple in Fig. 16A). Corresponding HI isolines range from 0 to 150 mg HC/g TOC and indicate kerogen types III and IV (inert) and low potential source rocks.

GP highly correlates with high HI and TOC contents (Fig. 16B). Marine contribution is indicative of source-rock generation. Terrestrial contribution is interpreted as best source rocks in the distal zone. It is assumed that higher detrital input supports: (i) higher nutrient flux and increase in primary productivity leading to increased carbon burial, and (ii) higher terrestrial organic matter input. Additionally, a transgressive event can prevent oxygenation and oxidation and help the preservation of organic matter. Kerogen types II and III of the outer shelf area favor gas and oil generation. Kerogen type II and the marine signature of the area in the middle shelf indicate generation of oil. Kerogen of the third area is inert or little gas prone.

The distribution of T_{max} is similar to that of the lower Paracuru Formation, but a decrease in values is observed. The absence of the 450 °C isotherm is interpreted as a decrease in tectonic activity (Fig. 16D). Mature kerogen delimited by T_{max} ranging from 435 to 465 °C corresponds to the oil window (Espitalié et al., 1984). The thickness of the sedimentary unit is relevant to reach minimum maturity conditions. Despite low GP values, a good match exists between TOC, HI and GP data, as seen in Fig. 16A–C and reinforces the previous interpretation related to kerogen type III or IV. Gas generation conditions are better in the outer shelf when compared to the middle shelf.

The Uruburetama Member is described as the transgressive member of the Ubarana Formation (Condé et al., 2007). Geochemical data are indicative of marine conditions in proximal areas. Distal areas located in the outer shelf are a little more promising, and mixing of marine end terrestrial kerogen types is assumed (Fig. 16C). Combined marine and terrestrial contributions are interpreted as relevant for TOC increase and may result from a greater input of terrigenous components to the basin. Transgressive conditions control the quality of the organic matter, affecting the sediments in a broader manner. The geochemical data distribution pointed to a marine signature in proximal areas of the middle shelf and the low potential of marine-terrestrial zones towards the land.

Regarding the Itapajé Member, TOC contents increase from southwest to northeast and basinward (Fig. 17A). The correlation between TOC and HI (Fig. 17A and C) defines two general patterns. The first pattern is characterized by TOC contents ranging from 0 to 1 wt% (represented in purple in Fig. 17A), which indicates poor or fair source-rock potential. HI values ranging from 1 to 50 mg HC/g TOC are indicative of kerogen type IV, which is interpreted as inert or with no potential for hydrocarbon generation, attesting the results obtained from Figs. 3 and 7. This low-TOC sequence is interpreted as highly reworked and of terrestrial origin or alternatively the burial and time for maturation were not attained.

An increase in TOC contents, ranging from 1 to 2.5 wt% and indicating a good potential for the source rocks, is observed in the second pattern, represented in green, yellow and red in Fig. 17A. HI also increases (from 75 to 150 mg HC/g TOC) and is interpreted as kerogen type III derived from terrestrial plant matter, indicating potential for gas generation. The terrestrial contribution widespread in the sedimentary succession is suggestive of basinward prograding events.

The T_{max} isoline map of Fig. 17D (see wells 3-AT-8, 1-CES-27, 1-CES-82 and 1-CES-44) shows two groups of T_{max} values that are neither oil nor gas prone. One group is characterized by T_{max} <430 °C (represented in green in Fig. 17D) and corresponds to immature kerogen, once maturation for hydrocarbon production starts at Tmax >430 °C. It is predominant in the middle shelf, where Tmax values vary from 400 to 434 °C. This behavior indicates shallower burial depths. However, the lack of Rock-Eval pyrolysis results (see wells 4-CES-14, 4-CES-21, 1-CES-45A, 1-CES-80 and 4-CES-12A) also can suggest immature kerogen. In the outer shelf (yellow and orange areas in Fig. 17D), T_{max} >500 °C, above the temperature of 465 °C at which over-maturation starts taking place. An increase in depth and over-mature rocks, with kerogen classified in the wet gas zone (Fig. 8B), confirm paleo-temperatures above 200 °C.

Under- or over-maturation conditions, as interpreted from temperature ranges, can be related to the sedimentary loads that were deposited on organic-rich sediments in deeper, more distal areas (represented in orange and yellow in Fig. 17D). This observation suggests a basinward prograding movement. A basinward movement of sediments a with terrestrial kerogen signature, plus low TOC contents and low HI values, point to an oxic environment for the Itapajé Member. The values remained similar to those indicating low maturity (i.e., younger strata), which implies that these strata contain reworked sedimentary material. These results, together with those previously shown, are related to a regressive event and exhibit significant large-scale variations for the Itapajé Member (Fig. 17).

6. Discussion

6.1. Distribution and characteristics of the organic-rich strata

During the deposition of the Mundaú Formation in the Aptian

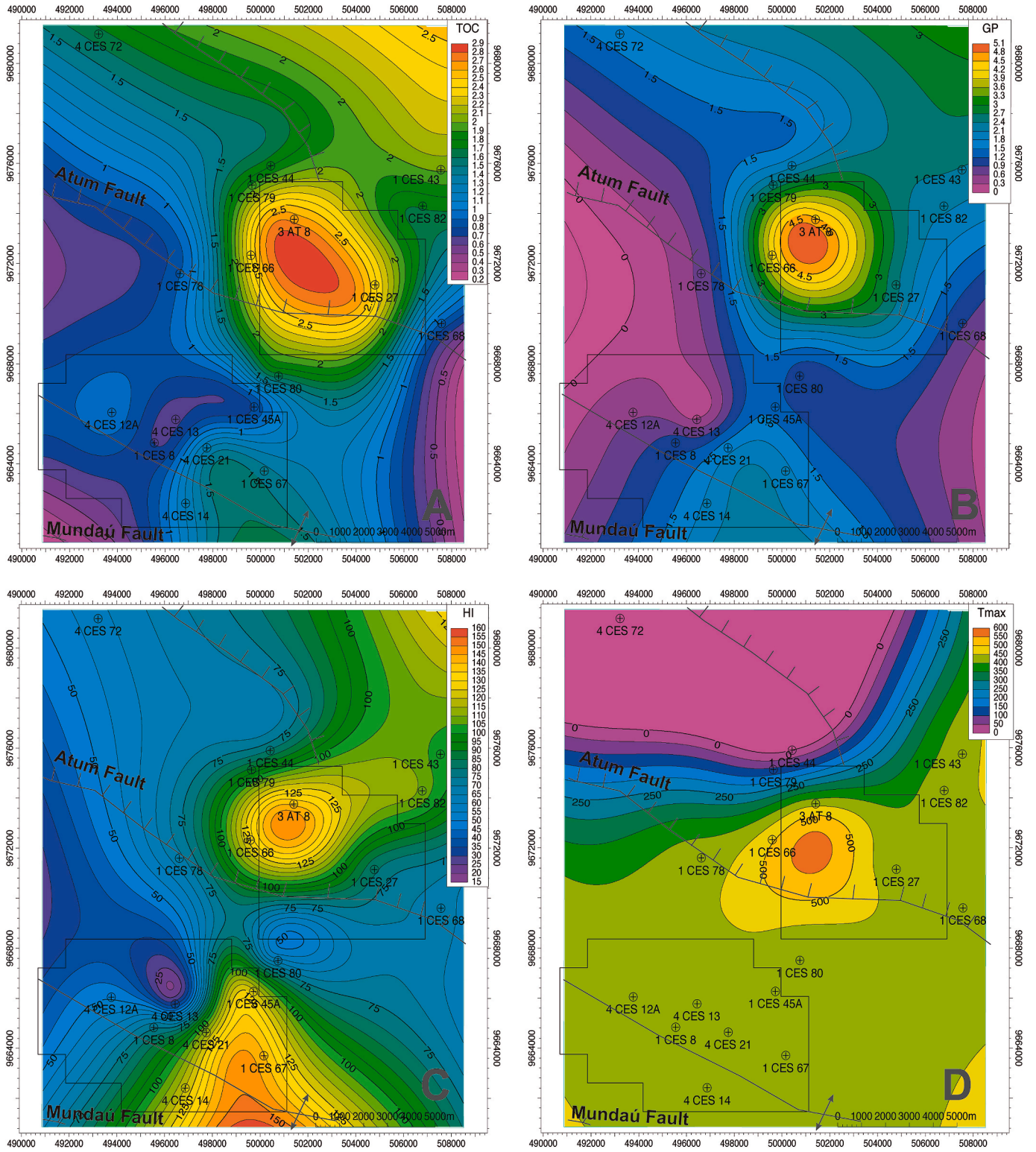

Fig. 17. Isoline maps for the characterization of the Itapajé Member source rocks. A) Spatial distribution based on mean TOC (wt. %) contents from line 4 to line 5 in Fig. 11 and 12. B) Genetic Potential (GP in mg HC/g rock). C) Hydrogen Index (HI in mg HC/g TOC). D) Temperatures at the peak of thermal cracking (T_{max}, in °C). T_{max}, GP and HI were calculated using mean values of Rock-Eval pyrolysis parameters obtained for 281 samples (Tables 1 and 2).

(Fig. 18A), active faults controlled the rifting of the basement, developing a series of horsts and grabens, in response to the transtensional tectonics (Pessoa Neto, 2004; Condé et al., 2007; Maia de Almeida et al., 2020b). The Ceará Basin contains a series of tilted blocks along NW-SE-trending *en echelon* normal faults (Szatmari et al., 1987; Matos 2000; Pessoa Neto, 2004; Maia de Almeida et al., 2020b). The NW-SE trending Mundaú and Atum faults are tectonic features that limit the study area (Fig. 1B) and activity along these structures controlled accommodation and consequent subsidence (Holz et al., 2017). In this sense, the isoline maps of Fig. 13 show that the best areas for oil generation in the Mundaú Formation are restricted to these fault-controlled areas (e.g., fault borders). This fault activity contributed to the increase

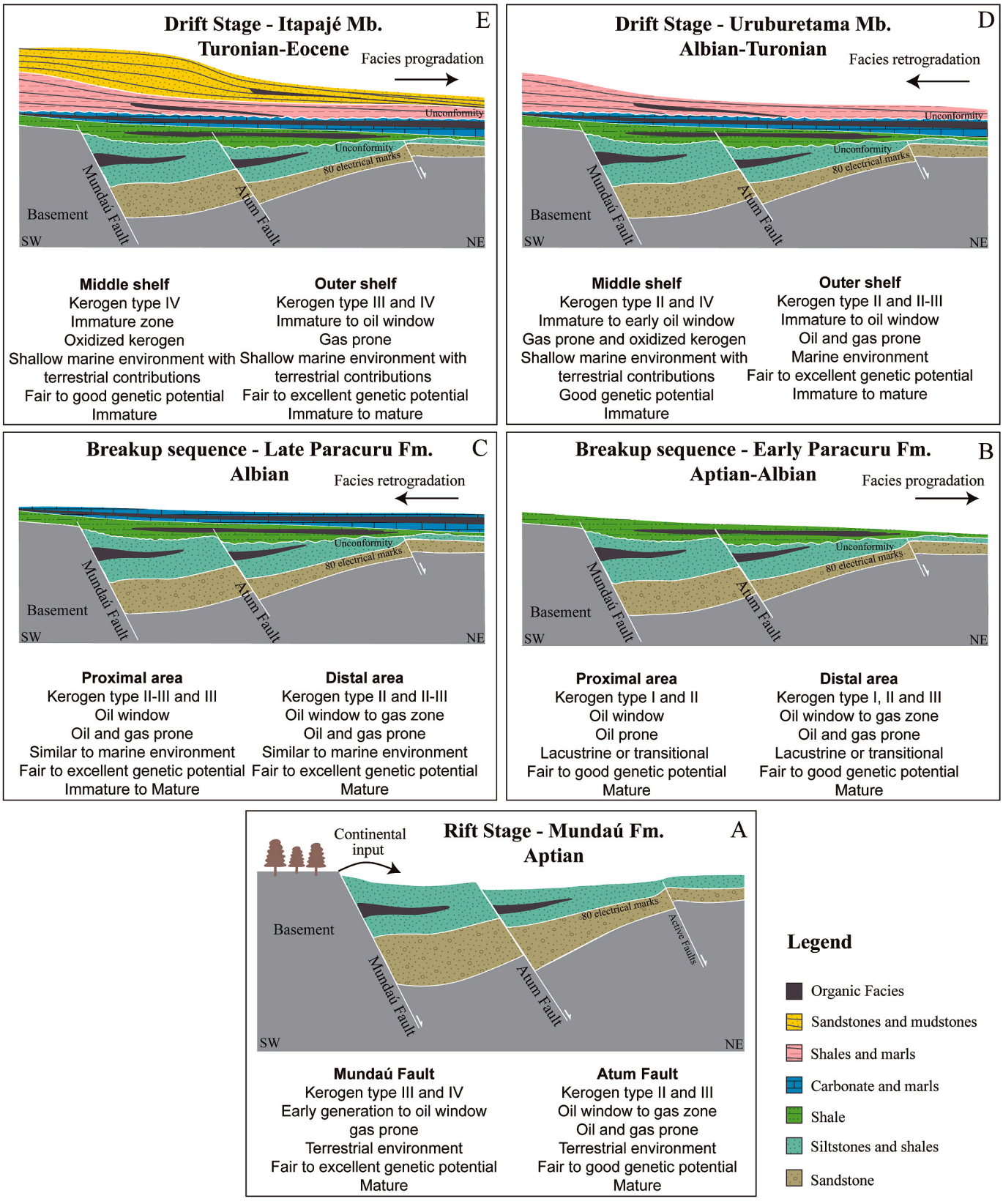

Fig. 18. Spatial distribution model of the source rocks the Ceará Basin in distinct tectonic regimes. The arrows indicate the main retrogradation and progradation directions related to the deposition of the source rocks and their geochemistry characteristics.

in accommodation space. The deposition of the best source rocks in the proximal region can be related to high sedimentation rates and organic matter availability. Thus, hydrocarbon generation and preservation can be correlated with the thickness of the sedimentary unit resulting from tectonic activity. The same applies to the Congo Basin, where the best source rocks are related to the rift-stage activity (Harris et al., 2005).

In these rift systems, source-rock sediments were deposited in fluvio-deltaic and lacustrine environments (Condé et al., 2007). The basins in these environments were infilled with terrestrial sediments, geochemically characterized in this study as kerogen type III (Figs. 4, 5, 8 and 9). The source rocks of the proximal areas are potential for gas generation and thermal maturity (Fig. 5A, B, 9A and 9B). However, in central to distal areas, TOC contents decrease, due to a decreased supply of terrestrial organic matter.

The breakup sequence sedimentation (Fig. 18B) is here informally divided in lower Paracuru and upper Paracuru formations. The lower Paracuru Formation is marked by basinward progradation facies. The first change with respect to the Mundaú Formation was the infill of estuaries and lagoons (resulting in kerogen types I and III), in reduced areas at the basin margins (e.g., Posamentier and Allen, 1999; Emery and Myers, 2009; Milton and Emery, 2009; Embry, 2012). The tectonic events that affected the Mundaú Formation did not interfere with the deposition of organic-rich sediments of the Paracuru Formation. Thus, kerogen types I and III are not spatially related to the footwalls.

A decrease in tectonic activity at the margins of the Ceará Basin suggests a decrease in terrestrial sediment input. However, fluvial discharges from the deltas brought nutrients to the basinal waters, favoring the organic input. The dataset previously described for the lower Paracuru Formation (see also Figs. 4, 5, 8, 9 and 14) suggests marine and deltaic contributions (Fig. 18B). The lower Paracuru Formation is a transitional sector of the Ceará Basin. The interaction of different paleoenvironments is marked by a wide range of kerogen types. Note that both environments, marine and terrestrial, are essential for the generation of source rocks. Genetic potential (S1 + S2) intersects these two areas (Fig. 14B). Fig. 14A and B (high TOC and GP values and predominance of kerogen types II and III) enhanced the moment of source rock generation. The low subsidence rates helped the preservation of abundant organic matter, characterized by immature to early oil-zone thermal conditions.

The main source rocks of the Ceará Basin were formed in the Late Albian (Figs. 15A and 18C). The upper Paracuru Formation is characterized by higher organic matter productivity (Fig. 18C). This result may be caused by more reducing environments (anoxia), and kerogen type II/III was produced under these conditions (Littke et al., 1988; Kosters et al., 2000). It is inferred that organic matter has a mixed marine-terrestrial origin. This result is similar to the proposed by Regali (1989), who proposed a marine ingression event correlated with the top layers of the Trairí Member. The upper Paracuru Formation represents retrogradation facies (Fig. 18C) characterized by black shales with high TOC contents (Figs. 11 and 12). The retrogradation is associated with milder tectonic activity as demonstrated by the relative regularity of the strata (Hashimoto et al., 1987) and preservation of organic matter. These interpretations help predict production characteristics for the proximal area similar or better than those of the distal areas, which is corroborated by the 2017 ANP Annual Report (ANP, 2017).

It was expected that the Ubarana Formation could constitute potential source rocks (Figs. 8 and 18D), additionally to the Mundaú and Paracuru formations, as described by Mello et al. (1984), Hashimoto et al. (1987), Cerqueira et al. (1994) and Condé et al. (2007). However, the source rocks of the Uruburetama and Itapajé members in the middle and outer shelves are not organic-rich (Fig. 18D and E). These members are less favorable to hydrocarbon generation, when compared to the Mundaú and Paracuru formations. On the other hand, geochemical indexes point to promising distal and deep-water areas, as suggested by Leopoldino Oliveira et al. (2020).

Considerable geochemical similarities are observed between the shelf and deep-water segments of the Ceará Basin. The Mundaú Formation contains type-III organic matter of terrestrial origin and is gas prone. The Paracuru Formation contains kerogen types I and II and subordinate type III, favorable to oil and gas generation. A source-rock interval was identified in deep-water regions by Maia de Almeida et al. (2020a) and Leopoldino Oliveira et al. (2020). These results suggest an extensive event of source-rock generation with marine organic matter deposited in reducing environments (Demaison and Moore 1980). The Ubarana Formation is less promising than the other formations, even if organic-rich strata exist in the sequence. However, thermal maturity has not been reached, as implied by the immature source-rock signature.

The deep-water approach reinforces the regional interpretation of our research for the Ubarana Formation (Leopoldino Oliveira et al., 2020). The 2017 ANP Annual Report showed that the oil reserves of the Xaréu field are 44.95 million cubic meters and of the Atum field, 24.9 million cubic meters (ANP, 2017). The difference is assigned to petroliferous systems. The difference in production in the Xaréu and Atum fields could be related to source rocks position, the quality of hydrocarbon generation, and the expulsion efficiency. All these features contribute to the differences in the migration processes.

6.2. Equatorial Margin correlation

In the following paragraphs, a comparison will be made between the Ceará Basin and other Equatorial Margin Basins. The Aptian Mundaú Formation, object of this study, consists of gas prone, terrestrial source rocks. The neighboring Pará-Maranhão and Barreirinhas basins do not correlate with such source-rock interval (Soares et al., 2007; Trosdtorf et al., 2007; Pellegrini and Ribeiro, 2018). The source rocks of the Potiguar Basin are related to the rift-phase Pendência Formation, deposited in lacustrine depositional systems, with kerogen types I and II, and gas prone (Trindade et al., 1992; Spigolon and Santos, 2005). The source rocks of the Guinea Gulf Province in the Equatorial Conjugate Margins of Africa were formed in the mid-Albian and are described as gas prone. Similar to the Mundaú Formation, organic matter is of terrestrial origin (Brownfield and Charpentier, 2006).

The main source rocks of the Ceará Basin are found in the Albian Paracuru Formation. In the Potiguar Basin, the Alagamar Formation is related to this time interval (Trindade et al., 1992; Condé et al., 2007). In the Guinea Gulf Basin, transgressive marine, oil-prone source rocks were also formed in the Albian (Brownfield and Charpentier 2006). These source rocks may also be correlated with the Late Albian-Early Cenomanian Caju Group of the Pará-Maranhão and Barreirinhas basins, which is composed of shales and calcilutites deposited in a transgressive marine depositional environment according to Soares et al. (2007) and Trosdtorf Jr. et al. (2007).

Potential Cenomanian-Turonian source rocks in the Ceará Basin are the Uruburetama and Itapajé members (Ubarana Formation). Rocks that reached thermal maturity are oil-prone marine shales, with kerogen types II and II-III. The Travosas Formation of the Pará-Maranhão and Barreirinhas basins is correlated with marine black shales related to anoxic events of the Cenomanian-Turonian (Soares et al., 2007; Trosdtorf et al., 2007). In the Guinea Gulf basin, this same time interval is marked by black shale deposition in anoxic oceanic conditions (Brownfield and Charpentier, 2006). Core samples from deep-sea drilling in both north and south parts of the Guinea Gulf Basin indicate that the source rocks contain more than 10% of organic matter consisting of kerogen type II. The same increase in TOC contents in deep waters was observed in the Turonian Ubarana Formation, which yielded more than 10% organic matter (Leopoldino Oliveira et al., 2020).

6.3. Expulsion and petroleum systems

The RHP vs. depth diagram concerning the middle shelf (Fig. 6B) indicates expulsion threshold at 1635 m, while in the outer-shelf, the

expulsion threshold is at 2106 m (Atum field – Fig. 10B), an in deep waters, at 3632 m (Fig. 10C). This difference can be explained by the proximity of the outer shelf to intrusive rocks and the greater thickness of the sedimentary units caused by overlying progradational deposits related to sand fans of the Tibau and Guamaré formations (Condé et al., 2007). Another parameter provided by the RHP vs. depth diagrams is the active source rock depth limit (ASDL), which marks the end of hydrocarbon generation. Thus, hydrocarbon exploration depth limit based on active source rocks of the middle shelf is 3500 m, and of the Atum field is 4500 m. These values could be used as a limit for oil exploration in the future. In deep waters, this value is 6000 m and is also a depth limit to new drillings.

Comparing with other source rocks of the Equatorial Margin, such depth limits for oil generation are compatible. In the Pará-Maranhão and Barreirinhas basin, the source rocks of the Late Albian-Early Cenomanian and Cenomanian-Turonian, for example, may be at 2400 m and 3700 m depths in shallow waters and from 1300 m to 4800 m beyond the faulted shelf border. In deep/ultra-deep waters, the Aptian source rocks are at 2860 m and 4550 m depths (Pellegrini and Ribeiro, 2018). Heat flow may increase in deep-water depths, as the continental crust is thinner, resulting in shallower generation thresholds.

According to the Strategic Research Center of Oil and Gas Resources (SRCOGR, 2009) and based on RHP data from other 16 sedimentary basins, the Ceará Basin is classified as a Strong Heat Flow Basin; in other words, it is characterized by a steep geothermal gradient, shallow source-rock generation, and strong compaction, leading to upward hydrocarbon migration, in order to form conventional reservoirs in traps. Expulsion can be related to the greater potential of conventional oil and gas storages to migrate from source rocks below these reservoirs (Pang et al., 2005; Wu et al., 2015; Xu et al., 2019). Leopoldino Oliveira et al. (2020) have recently discussed the heat flow history of the Ceará Basin.

The parameters extracted from the RHP vs. depth diagram (e.g., ASDL and expulsion threshold) are useful to understand thermal maturity in basin modeling. Additionally, heat flow can be evaluated based on the sedimentary basin tectonic evolution and rifting phase (Allen and Allen, 1990). Rifting and lithospheric thinning influence the heat flow inside the basin. Heat is incorporated during rifting, but exponential reduction takes place during post-rift stages (McKenzie, 1978). The identification of sills in seismic profiling (Leopoldino Oliveira et al., 2020) related to submerged volcanic seamounts (Rios and Picanço, 2019; Maia de Almeida et al., 2020a,b; Leopoldino Oliveira et al., 2020; Mohriak, 2020), and the presence of intrusive rocks along the Romanche Transform Zone and in deep/ultra-deep waters may favor maturation. These results corroborate the classification of the Ceará Basin setting as of Passive Margin with Active Volcanism (Abreu, 1998; Zalán, 2015; Leopoldino Oliveira et al., 2020).

7. Conclusions

The geochemical parameters analyzed in this study suggest for the Mundaú Formation (rift phase) moderate to good potential for oil generation and good potential for gas generation. Thermal maturity is high, being the source rocks thermally mature to over-mature. The main source rocks are associated with fault systems. The source rocks capable of generating hydrocarbons are deeply buried. High TOC contents are observed in proximal regions, which reflect high primary productivity. Lateral changes in the Mundaú Formation are related to fault borders that were active during rifting, favoring sediment supply for source-rock generation. Kerogen is predominantly of types III and IV. Kerogen type III and reworked organic matter are predominant in shallower portions and probably result from major terrestrial contributions to the basin.

Good to excellent source rocks are characteristic of the Paracuru Formation (breakup sequence). Kerogen types I and II predominate, with subordinate type III and mixed kerogen. The variety of kerogen types indicates transitional environments. The most organic-rich source rocks are related to this interval. This unit is thermally mature, and it is oil and gas prone. Reduced tectonic activity, marine ingression, and restricted environments may have influenced the potential for oil generation. The Paracuru Formation in deep waters is oil and gas prone. These results suggest an extensive event of source-rock formation with marine organic matter deposited in reducing conditions. The upper Paracuru Formation is a significant contribution to the Ceará Basin source-rock potential and the most promising interval for hydrocarbon generation. This relatively thin interval ranges from the top of the Trairí Member to the top of the Paracuru Formation.

The potential of the Uruburetama Member of the Ubarana Formation (drift phase) to generate oil is moderate to good. Source rocks are located in proximal regions and were deposited under reducing conditions in a transgressive marine environment. Distal areas in the outer shelf are slightly more promising. The mixing of marine and terrestrial kerogen is assumed to be relevant for the increase of TOC contents and probably results from a greater contribution of terrestrial components into the basin. T_{max} values indicate immature to mature kerogens in proximal and the distal regions, respectively. These results are more promising for samples of the oil window/zone (e.g., PI vs. T_{max} diagram). Kerogen encompasses type II, a mixture of types II and III, and subordinate type III. The Uruburetama Member is oil and gas prone.

The organic matter of the proximal areas of the Itapajé Member is of low quality and relative scarce. TOC and S2 values suggest poor to fair potential for oil generation. Kerogen type IV (inert or degraded) is typical in the middle shelf, and kerogen type IV and subordinate type III are typical in the outer shelf. The presence of inert kerogen is related to high-energy, oxidizing depositional environments. Terrestrial kerogen in distal regions corroborates the interpretation of regressive events in the Ceará Basin. Source rocks are predominantly immature to marginally mature. These results indicate that the Itapajé Member may not have attained the maturation to generate hydrocarbons. Great similarities were observed between shelf and deep-water areas in the Ceará Basin. The Ubarana Formation is the least promising source rock, despite organic-rich strata have been detected in distal regions.

The hydrocarbon expulsion threshold and active source rock depth limit (ASDL) were used in this study to determine the thermal conditions in the Ceará Basin, which is characterized as a strong heat flow basin; in other words, steep geothermal gradient, shallow source-rock generation, and strong compaction. These characteristics favor the conventional accumulation of hydrocarbons, which migrate upwards to form conventional reservoirs. Their expulsion from source rocks can be related to a greater potential to generate conventional oil and gas storages and corroborate the recent classification of the Ceará Basin setting as Passive Margin with Active Volcanism.

Credit author statement

Ana Clara B. Souza: Conceptualization, data curation, investigation, formal analysis, visualization, writing - original draft, review and editing. Daniel R. do Nascimento Jr: Supervision, visualization, validation, writing - review and editing; Alessandro Batezelli: Supervision, visualization, validation, writing - review and editing. Francisco Nepomuceno Filho: Supervision, visualization, validation, project administration, funding acquisition, resources, writing - review and editing. Karen M. Leopoldino Oliveira: Data curation, formal analysis, visualization, writing - review and editing. Narelle M. de Almeida: Formal analysis, visualization, writing - review and editing. Márcio Nunes Normando: writing - review and editing. Thiago Henrique da Silva Barbosa: Data curation, formal analysis, writing - review and editing.

Declaration of competing interest

The authors declare that they have no known competing financial interests or personal relationships that could have appeared to influence the work reported in this paper.

Acknowledgements

We would like to thank the National Agency of Petroleum, Natural Gas and Biofuels (ANP) for providing the geochemistry data. We thank Schlumberger for ceded the Petrel E&P software licenses. We thank the Laboratory of Seismic Interpretation of the Federal University of Ceará for the infrastructure available to support this research. The authors are also grateful to the anonymous reviewers for their constructive comments. We are grateful to Gianna Garda for her English proofreading and general comments. This study was financed in part by the Brazilian Council Coordination (Coordenação de Aperfeiçoamento de Pessoal de Nível Superior - Brazil (CAPES) - Finance Code 001).

References

Abreu, V.S., 1998. Geologic Evolution of Conjugate Volcanic Passive Margins: Pelotas Basin (Brazil) and Offshore Namibia (Africa). Implication for Global Sea Level Changes. Diss.. Rice University https://hdl.handle.net/1911/19338.

Allen, P.A., Allen, J.R., 1990. Basin Analysis: Principles and Application to Petroleum Play Assessment. John Wiley & Sons.

Almeida, F.F.M. De, Brito Neves, B.B. De, Dal Ré Carneiro, C., 2000. The origin and evolution of the South 1491 American platform. Earth Sci. Rev. 50, 77–111. https://doi.org/10.1016/S0012-987 8252(99)00072-0.

Anders, D., 1991. Geochemical Exploration Methods: Chapter 7: Geochemical Methods and Exploration. Book Title: Source and Migration Processes and Evaluation Techniques, pp. 89–95. https://doi.org/10.1306/TrHbk543C7.

ANP, 2017. Bacia do Ceará - Sumário Geológico e Setores em Oferta 21.

Aplin, A.C., Macquaker, J.H.S., 2011. Mudstone diversity: origin and implications for source, seal, and reservoir properties in petroleum systems. American Association of Petroleum Geologists. Bull. (Arch. Am. Art) 95, 2031–2059. https://doi.org/10.1306/03281110162.

Azevedo, R.P., 1991. Interpretation of a deep seismic reflection profile in the Pará-Maranhão Basin. In: Congresso Internacional da Sociedade Brasileira de Geofísica, vol. 2, pp. 661–666. https://doi.org/10.3997/2214-4609-pdb.316.122. Salvador-BA, Anais.

Babakhani, M., 2018. Uncertainty analysis in geological surface modelling. In: AAPG Poster, p. 4999.

Barker, C., 1974. Pyrolysis techniques for source-rock evaluation. AAPG Bull. (American Assoc. Pet.Geol.) 58, 2349–2361. https://doi.org/10.1306/83D91BAF-16C7-11D7-8645000102C1865D.

Behar, F., Beaumont, V., De, B., Penteado, H.L., 2001. Rock-eval 6 technology: performances and developments. Oil Gas Sci. Technol. 56, 111–134. https://doi.org/10.2516/ogst:2001013.

Beltrami, C.V., Alves, L.E.M., Feijó, F.J., 1994. Bacia do Ceará. Boletim de. Geociencias da Petrobrás 8, 117–125.

Bordenave, M.L., Espitalié, J., Leplat, P., Oudin, J.L., Vandenbroucke, M., 1993. Screening Techniques for Source Rock Evaluation. Applied Petroleun, Geochemistry.

Brownfield, M.E., Charpentier, R.E., 2006. Geology and total petroleum systems of the Gulf of Guinea Province of West Africa. U.S Geological Survey Bulletin 2207-C, p. 32.

Cerqueira, J.R., Soldan, A.L., Mello, M.R., Beltrami, C.V., 1994. Identificacao das Rochas Geradoras de Hidrocarbonetos da Bacia do Ceará. XXXIII Congresso. Brasileiro de Geoleologia.

Condé, V.C., Lana, C.C., Da Cruz Pessoa Neto, O., Roesner, E.H., De Morais Neto, J.M., Dutra, D.C., 2007. Bacia do Ceará. Boletim de. Geociencias da Petrobrás 15, 347–355.

Cornford, C., 1979. Organic Deposition at a Continental Rise: Organic Geochemical Interpretation and Synthesis at DSDP Site 397, Eastern North Atlantic. Initial Reports Deep Sea Drill. Proj. Part. 1 Washingt. (US Gov. Off, pp. 503–510.

Costa, I.G., Beltrami, C.V., e Alves, L.E.M., 1990. A Evolução Tectono-Sedimentar e o Habitat do Óleo da Bacia do Ceará. Bol. Geociencias Petrobras 4, 65–74.

Coutinho, P.N., Morais, J.O., 1968. Distribuicion de lós Sedimentos en la plataforma continental norte y nordeste del Brasil. In: Curaçao UNESCO (Ed.), Symposium on Investigation and Resources of the Caribbean Sea and Adjacents Regions, pp. 313–315. Extended Abstract.

Curiale, J.A., 2008. Oil-source rock correlations - limitations and recommendations. Org. Geochem. 39, 1150–1161. https://doi.org/10.1016/j.orggeochem.2008.02.001.

Curiale, J.A., Cole, R.D., Witmer, R.J., 1992. Application of organic geochemistry to sequence stratigraphic analysis: four corners platform Area, New Mexico, U.S.A. Org. Geochem. 19 https://doi.org/10.1016/01466380(92)90027-U.

Davison, I., Faull, T., Greenhalgh, J., O Beirne, E., Steel, I., 2016. Transpressional structures and hydrocarbon potential along the Romanche Fracture Zone: a review. Geol. Soc. Lond. Spec. Publ. 431, 235–248. https://doi.org/10.1144/sp431.2.

Demaison, G.J., Moore, G.T., 1980. Anoxic environments and oil source rock bed genesis. AAPG (Am. Assoc. Pet. Geol.) Bull. 64, 1179–1209.

Dembicki, H., 2009. Three common source rock evaluation errors made by geologists during prospect or play appraisals. American Association of Petroleum Geologists. Bulletin 93, 341–356. https://doi.org/10.1306/10230808076.

Embry, A.F., 2012. Transgressive-regressive (T-R) sequence stratigraphy. Seq. In: Stratigr. Model. Explor. Prod. Evol. 1563 Methodol. Emerg. Model. Appl. Hist. 22nd Annu., pp. 151–172. https://doi.org/10.5724/gcs.02.22.0151.

Emery, D., Myers, K. (Eds.), 2009. Sequence Stratigraphy. John Wiley & Sons.

Espitalié, J., Laporte, J.L., Madec, M., Marquis, F., Leplat, P., Paulet, J., Boutefeu, A., 1977. Rapid method for source rocks characterization and for determination of petroleum potential and degree of evolution. Rev. Institut Français du Pétrole. 32, 23–42. https://doi.org/10.2516/ogst:1977002.

Espitalié, J., Marquis, F., Barsony, I., 1984. In: Voorhees, K.J.B.T.-A.P. (Ed.), 9 - GEOCHEMICAL LOGGING. Butterworth-Heinemann, pp. 276–304. https://doi.org/10.1016/B978-0-408-01417-5.50013-5.

Fang, H., Jianyu, C., Yongchuan, S., Yaozong, L., 1993. Application of organic facies studies to sedimentary basin analysis: a case study from the Yitong Graben, China. Org. Geochem. 20, 27–42. https://doi.org/10.1016/0146-6380(93)90078-.

Fujie, J., Pang, X., Jing, B., Xinhuai, Z., Jianping, L., Yonghua, G., 2016. Comprehensive assessment of source rocks in the Bohai Sea area, eastern China. AAPG (Am. Assoc. Pet. Geol.) Bull. 100 (6), 969–1002. https://doi.org/10.1306/02101613092.

Harris, N.B., 2005. The deposition of organic-carbon-rich sediments: models, mechanisms, and consequences introduction. Depos. Org. Sediments Model. Mech. Consequences. https://doi.org/10.2110/pec.05.82.0001.

Harris, N.B., Freeman, K.H., Pancost, R.D., Mitchell, G.D., White, T.S., Bate, R.H., 2005. Patterns of Organic-Carbon Enrichment in a Lacustrine Source Rock in Relation to Paleo-Lake Level. CongoBasin, West Africa. https://doi.org/10.2110/pec.05.82.0103.

Hart, B.S., Steen, A.S., 2015. Programmed Pyrolysis (Rock-Eval) Data and Shale Paleoenvironmental Analyses: A Review. Interpretation 3, SH41–SH58. https://doi.org/10.1190/INT-2014-0168.1.

Hashimoto, A.T., Appi, C.J., Soldan, A.L., Cerqueira, J.R., 1987. The Neo-Alagoas in the Ceara, Araripe and Potiguar basins (Brazil): stratigraphic and paleoecological characterization. Rev. Bras. Geociencias 17, 118–122.

Heine, C., Brune, S., 2014. Oblique rifting of the equatorial atlantic: why there is no saharan atlantic ocean. Geology 42, 211–214. https://doi.org/10.1130/G35082.1.

Holz, M., Vilas-Boas, D.B., Troccoli, E.B., Santana, V.C., Vidigal-Souza, P.A., 2017. Conceptual models for sequence stratigraphy of continental rift successions. Stratigr. Timescales 2, 119–186. https://doi.org/10.1016/bs.sats.2017.07.002.

Horsfield, B., Curry, D.J., Bohacs, K., Littke, R., Rullkötter, J., Schenk, H.J., et al., 1994. Of the washakie basin, Wyoming, USA. Org. Geochem. 22 (3–5), 415–440. https://doi.org/10.1016/0146-6380(94)90117-1.

Hunt, J.M., 1995, second ed.. Petroleum Geochemistry and Geology. https://doi.org/10.1017/S0016756800007755 743 pp ISBN 0 7167 2441 3. 133(4), Second Edition, 743 pp.

Jacob, H., 1989. Classification, structure, genesis and practical importance of natural solid oil bitumen ("migrabitumen"). Int. J. Coal Geol. 11, 65–79.

Jarvie, D.M., 1991. Total organic carbon (TOC) analysis. Chapter 11: geochemical methods and exploration. In: Book Title: Source and Migration Processes and Evaluation Techniques, pp. 113–118. https://doi.org/10.1306/TrHbk543C11.

Jarvie, D.M., 2012. Shale resource systems for oil resource systems. Shale-oil resource systems. In: Breyer, n J.A. (Ed.), Shale Reservoirs—Giant Resources for the 21st Century. AAPG Memoir, pp. 89–119. https://doi.org/10.1306/13321447m973489.

Jarvie, D.M., Lundell, L.L., 2001. Chapter 15: amount, type, and kinetics of thermal transformation of organic matter in the Miocene Monterey Formation. In: The Monterey Formation: from Rocks to Molecules, Caroline M. Isaacs and Jurgen Rullkotter. Columbia University Press, pp. 268–295.

Katz, B.J., 1983. Limitations of 'Rock-Eval' pyrolysis for typing organic matter. Org. Geochem. 4, 195–199. https://doi.org/10.1016/0146-6380(83)90041-4.

Katz, B.J., 2005. Controlling factors on source rock development—a review of productivity, preservation, and sedimentation rate. Depos. Org. Sediments Model. Mech. Consequences. https://doi.org/10.2110/pec.05.82.0007.

Kolonic, S., Wagner, T., Forster, A., Sinninghe Damsté, J.S., Walsworth-Bell, B., Erba, E., Turgeon, S., Brumsack, H.J., Chellai, E.H., Tsikos, H., 2005. Black shale deposition on the northwest African Shelf during the Cenomanian/Turonian oceanic anoxic event: climate coupling and global organic carbon burial. Paleoceanography 20, PA1006. https://doi.org/10.1029/2003PA000950.

Kosters, E.C., VanderZwaan, G.J., Jorissen, F.J., 2000. Production, preservation and prediction of source-rock facies in deltaic settings. Int. J. Coal Geol. 43 (1–4), 13–26.

Lana, C.C., Arai, M., Roesner, E.H., 2002. Dinoflagelados fósseis da seção cretácea marinha das bacias marginais brasileiras: um estudo comparativo entre as margens equatorial e sudeste. Simpósio sobreo Cretáceo do Brasil 6, 247–252.

Langford, F.F., Blanc-Valleron, M.M., 1990. Interpreting rock-eval pyrolysis data using graphs of pyrolizable hydrocarbons vs. Total organic carbon. AAPG (Am. Assoc. Pet. Geol.) Bull. 74 doi:10.1306/0c9b238f- 1710-11d7-8645000102c1865d.

Leopoldino Oliveira, K.M., Bedle, H., Branco, R.M.G.C., de Souza, A.C.B., Nepomuceno Filho, F., Nomando, M.N., de Almeida, N.M., da Silva Barbosa, T.H., 2020. Seismic stratigraphic patterns and characterization of deepwater reservoirs of the Mundaú sub-basin, Brazilian Equatorial Margin. Mar. Petrol. Geol. https://doi.org/10.1016/j.marpetgeo.2020.104310.

Li, M., Yao, H., Stasiuk, L.D., Fowler, M.G., Larter, S.R., 1997. Effect of maturity and petroleum expulsion on 1644 pyrrolic nitrogen compound yields and distributions in Duvernay Formation petroleum source rocks in central 1645 Alberta, Canada. Org. Geochem. 26, 731–744. https://doi.org/10.1016/S0146-6380(97)00053-3.

Littke, R., Baker, D.R., Leythaeuser, D., 1988. In: Mattavelli, L., Novelli, L.B.T.-O.G.I.P.E. (Eds.), Microscopic and Sedimentologic Evidence for the Generation and Migration of Hydrocarbons in Toarcian Source Rocks of Different Maturities. Pergamon, Amsterdam, pp. 549–559. https://doi.org/10.1016/B978-0-08-037236-5.50061-0.

Magoon, L.B., Dow, W.G., 1994. The Petroleum System: from Source to Trap: AAPG Memoir 60. American Association of Petroleum Geologists, Tulsa, pp. 25–49. ISBN: 1588613763.

Maia de Almeida, N., Alves, T.M., Nepomuceno Filho, F., Freire, G.S.S., Souza, A.C.B. de, Normando, M.N., Oliveira, K.M.L., Barbosa, T.H. da S., 2020a. Tectono-sedimentary evolution and petroleum systems of the Mundaú sub-basin: a new deep-water

exploration frontier in equatorial Brazil. Am. Assoc. Petrol. Geol. Bull. 104, 795–824. https://doi.org/10.1306/07151917381.
Maia de Almeida, N., Alves, T.M., Nepomuceno Filho, F., Freire, G.S.S., Souza, A.C.B., Leopoldino Oliveira, K.M., Normando, M.N., Barbosa, T.H.S., 2020b. A three-dimensional (3D) structural model for an oil-producing basin of the Brazilian Equatorial margin. Mar. Petrol. Geol. https://doi.org/10.1016/j.marpetgeo.2020.104599, 104599.
Mascle, J., Blarez, E., Marinho, M., 1988. The shallow structures of the Guinea and Ivory Coast-Ghana transform margins: their bearing on the Equatorial Atlantic Mesozoic evolution. Tectonophysics 155, 193–209. https://doi.org/10.1016/0040-1951(88)90266-1.
Matos, R.M.D., 2000. Tectonic evolution of the equatorial South Atlantic. Atlantic Rifts Continental Margins 115, 331–354. https://doi.org/10.1029/GM115p0331.
McKenzie, D., 1978. Some remarks on the development of sedimentary basins. Earth Planetary Sci. Lett. Elsevier Sci. Publ. Company Amsterdam 40 (1), 25–32.
Mello, M.R., Soldan, A.L., Cerqueira, R.N., Beltrami, C.V., 1984. Avaliação geoquímica da Bacia do Ceará. Petrobrás/Cenpes (Relatório interno), Rio de Janeiro, p. 1663.
Mello, M.R., Telnaes, N., Gaglianone, P.C., Chicarelli, M.I., Brassell, S.C., Maxwell, J.R., 1988. Organic geochemical characterisation of depositional palaeoenvironments of source rocks and oils in Brazilian marginal basins. Org. Geochem. 13, 31–45. https://doi.org/10.1016/0146-6380(88)90023- X.
Milton, N.J., Emery, D., 2009. Outcrop and well data. In: Sequence Stratigraphy, pp. 61–79. https://doi.org/10.1002/9781444313710.ch4.
Mohriak, W.U., 2020. Genesis and evolution of the South Atlantic volcanic islands offshore Brazil. Geo Mar. Lett. 1–33. https://doi.org/10.1007/s00367-019-00631-w.
Mohriak, W.U., Rosendahl, B.R., 2003. Transform zones in the South Atlantic rifted continental margins. Geol. Soc. Lond. Spec. Publ. 210, 211–228. https://doi.org/10.1144/GSL.SP.2003.210.01.13.
Morais Neto, J.M., Pessoa Neto, O.C., Lana, C.C., Zalán, P.V., 2003. Bacias sedimentares brasileiras–Bacia do Ceará. Fundação Paleontológica Phoenix 57, 1–6.
Omodeo-Salé, S., Suárez-Ruiz, I., Arribas, J., Mas, R., Martínez, L., Josefa Herrero, M., 2016. Characterization of the source rocks of a paleo-petroleum system (Cameros Basin) based on organic matter petrology and geochemical analyses. Mar. Petrol. Geol. 71, 271–287. https://doi.org/10.1016/j.marpetgeo.2016.01.002.
Pang, X., Li, M., Li, S., Jin, Z., 2005. Geochemistry of petroleum systems in the Niuzhuang south slope of Bohai Bay basin: Part 3. Estimating hydrocarbon expulsion from the shahejie formation. Org. Geochem. 36 (4), 497–510. https://doi.org/10.1016/j.orggeochem.2004.12.0011152.
Pang, X., Jia, C., Zhang, K., Li, M., Wang, Y., Peng, J., Li, B., Chen, J., 2019. The depth limit for the formation and occurrence of fossil fuel resources. Earth Syst. Sci. Data Discuss. 1–26. https://doi.org/10.5194/essd-2019-72.
Pellegrini, B. da S., Ribeiro, H.J.P.S., 2018. Exploratory plays of Pará-Maranhão and Barreirinhas basins in deep and ultra-deep waters, Brazilian Equatorial Margin. Brazilian J. Geol. 48, 485–502. https://doi.org/10.1590/2317-4889201820180146, 1154.
Pessoa Neto, O.C., 2004. Blocos basculados truncados por discordância angular: lições aprendidas em trapeamento combinado de hidrocarbonetos, Bacia do Ceará, Nordeste do Brasil. Boletim de Geociencias da Petrobras v 12, 59–71.
Pessoa Neto, O. da C., Soares, U.M., Silva, J.G.F. da, Roesner, E.H., Florencio, C.P., Souza, C.A.V. de, 2007. Bacia potiguar. Bol. Geociencias Petrobras 15, 357–369.
Peters, K.E., 1986. Guidelines for evaluating petroleum source rock using programmed pyrolysis. Am. Assoc. Pet. 1709 Geol. Bull. 70, 318–329. https://doi.org/10.1306/94885688-1704-11D7- 8645000102C1865D.
Peters, K.E., Cassa, M.R., 1994. Applied source rock geochemistry. In: Magoon, L.B., Dow, W.G. (Eds.), The Petroleum System—From Source to Trap: Tulsa, Okla, vol. 60. American Association of Petroleum Geologists Memoir, pp. 93–117.
Peters, K.E., Kontorovich, A.E., Moldowan, J.M., Andrusevich, V.E., Huizinga, B.J., Demaison, G.J., Stasova, O.F., 1993. Geochemistry of selected oils and rocks from the central portion of the west Siberian basin, Russia1. Am. Assoc. Pet. Geol. Bull. 77, 863–887. https://doi.org/10.1306/BDFF8D80-1718-11D7-8645000102C1865D.
Peters, K.E., Magoon, L.B., Bird, K.J., Valin, Z.C., Keller, M.A., 2006. North Slope, Alaska: source rock distribution, richness, thermal maturity, and petroleum charge. Am. Assoc. Petrol. Geol. Bull. 90, 261–292. https://doi.org/10.1306/09210505095.
Peters, K.E., Magoon, L.B., Valin, Z.C., Lillis, P.G., 2007. Source-rock geochemistry of the san Joaquin basin Province, California. In: Chapter 11 in Petroleum Systems and Geologic Assessment of Oil and Gas in the San Joaquin Basin Province, California (No. 1713-11). US Geological Survey.
Posamentier, H.W., Allen, G.P., 1999. Siliciclastic Sequence Stratigraphy: Concepts and Applications, vol. 7. SEPM (Society for Sedimentary Geology, Tulsa, Oklahoma, p. 210. https://doi.org/10.13140/RG.2.1.3899.1124.
Regali, M.S., 1989. A idade dos evaporitos da plataforma continental do Ceará, Brasil e sua relação com os outros evaporitos das Bacias Nordestinas. Boletim IG-USP. Publicação Especial (7), 139–143. https://doi.org/10.11606/issn.2317-8078.v0i7p139-143.
Rios, I.L.A., Picanço, J. de J.F., 2019. Arcabouço Estratigráfico da Seção Drifte em Águas Profundas da Sub-Bacia de Mundaú, Bacia do Ceará, e sua Relação com a Datação de Eventos Vulcânicos. Anuário do Instituto de Geociências 41 (2), 152–166. https://doi.org/10.11137/2018_2_152_166.
Rullkötter, J., Cornford, C., Welte, D.H., 1982. Geochemistry and petrography of organic matter in northwest 1719 African continental margin sediments: quantity, provenance, depositional environment and temperature 1720 history. Geol. Northwest African Cont. Margin 50, 686–703. https://doi.org/10.1007/978-3-642-68409-8_28.
Silva Filho, W.F.D., Castro, D.L., Corrêa, I.C.S., Freire, G.S.S., 2007. Estruturas Rasas na Margem Equatorial ao Largo do Nordeste Brasileiro (Estado do Ceará): análise de Relevo e Anomalias Gravimétricas Residuais. Rev. Bras. Geofís. 25, 65–77.
Soares, E.F., Zalán, P.V., Figueiredo, J.J.P., Trosdtorf Jr., I., 2007. Bacia do pará-maranhão. Bol. Geociencias Petrobras 15 (2), 321–330.
Spigolon, A.L.D., Santos, N., 2005. Geoquímica Orgânica do Eocretáceo da Bacia Potiguar: Implicações Paleoambientais e Paleoclimáticas. In: Congresso Brasileiro de Geoquímica, vol. 10, pp. 14–514.
SRCOGR, 2009. Strategic Research Center of Oil and Gas Resources, Ministry of Land and Resources) A New Round Hydrocarbon Resource Assessment for Whole China. China Land Press, Beijing.
Szatmari, P., Françolin, J.B.L., Zanotto, O., Wolff, S., 1987. Evolução Tectônica da Margem Equatorial Brasileira. Rev. Bras. Geociencias 17 (2), 180–188.
Tang, L., Pang, X., Song, Y., Jiang, Z., Jiang, S., Li, Q., Li, X., 2019. Lower limit of hydrocarbon generation in source rocks: a case study from the Dongpu Depression, Bohai Bay Basin, East China. J. Asian Earth Sci. https://doi.org/10.1016/j.jseaes.2019.103928, 103928.
Tissot, B.P., Welte, D.H., 1984. Petroleum formation and occurrence. Springer Science & Business Media. Berlin, 699. Part II, Chapter 1. ISBN 364287813XTyson, R. V., 2001. Sedimentation rate, dilution, preservation and total organic carbon: some results of a modelling 1758 Study. Org. Geochem. 32, 333–339. https://doi.org/10.1016/S0146-6380(00)00161- 3.
Tissot, B.P., Pelet, R., Ungerer, P.H., 1987. Thermal history of sedimentary basins, maturation indices, and kinetics of oil and gas Generation 1. Am. Assoc. Petrol. Geol. Bull. 71, 1445–1466. https://doi.org/10.1306/703C80E7-1707-11D7-8645000102C1865D.
Trindade, L.A.F., Brassell, S.C., Neto, E.S., 1992. Petroleum migration and mixing in the Potiguar Basin, Brazil. AAPG Bull. 76 (12), 1903–1924.
Trosdtorf Jr., I., Zalán, P.V., Figueiredo, J.J.P., Soares, E., 2007. Bacia de Barreirinhas. Bol. Geociencias Petrobras 15 (2), 331–339.
Van Krevelen, D.W., 1961. Coal: Typology, Chemistry, Physics. Constitution, 3. ISBN 9780444895868.
Waples, D.W., 1994. Maturity modeling: thermal indicators, hydrocarbon generation, and oil 1219 cracking. In: Chapter: Part IV. Identification and Characterization in: the Petroleum System—From 1220 Source to Trap. The Petroleum System–From Source to Trap.
Wu, L., Pang, X., Zhou, L., Pang, H., 2015. The quality evaluation and hydrocarbon generation and Expulsion characteristics of permian lucaogou Formation source rocks in Jimusar Sag, Junggar Basin. Acta Geologica Sinica (Engl. Ed. 89, 283–286 (supp.).
Xu, Z., Liu, L., Liu, B., Wang, T., Zhang, Z., Wu, K., Shu, Y., 2019. Geochemical characteristics of the Triassic Chang 7 lacustrine source rocks, Ordos Basin, China: implications for paleoenvironment,petroleum potential and tight oil occurrence. J. Asian Earth Sci. 178, 112–138. https://doi.org/10.1016/j.jseaes.2018.03.005.
Zalán, P.V., 2015. Similarities and differences between magma-poor and volcanic passive margins –applications to the Brazilian marginal basins. In: Conference Paper - 14th International Congress of the Brazilian Geophysical Society held in Rio de Janeiro, pp. 37–42. https://doi.org/10.1190/sbgf 2015-007. Brazil.
Zalán, P.V., Nelson, E.P., Warme, J.E., Davis, T.L., 1985. The Piaui Basin Rifting and Wrenching in an Equatorial Atlantic Transform Basin.